Multipoint targeting of TGFβ-Wnt transactivation circuit with microRNA 384-5p for cardiac fibrosis

Hyang-Hee Seo

Department of Medical Science
The Graduate School, Yonsei University

Multipoint targeting of TGFβ-Wnt transactivation circuit with microRNA 384-5p for cardiac fibrosis

Directed by Professor Jong-Chul Park

The Doctoral Dissertation
submitted to the Department of Medical Science,
the Graduate School of Yonsei University
in partial fulfillment of the requirements for the
degree of Doctor of Philosophy

Hyang-Hee Seo

December 2017

This certifies that the Doctoral Dissertation of Hyang-Hee Seo is approved.

Thesis Supervisor: Jong-Chul Park

Thesis committee Member #1: Ki-Chul Hwang

Thesis committee Member #2: Sahng Wook Park

Thesis committee Member #3: Gyoon-Hee Han

Thesis committee Member #4: Sang Kil Lee

The Graduate School

Yonsei University

December 2017

ACKNOWLEDGEMENTS

First and foremost, I would like to express the deepest appreciation to the members of the advisory committee, Prof. Jong-Chul Park, Prof. Ki-Chul Hwang, Prof. Sahng Wook Park, Prof. Gyoon-Hee Han and Prof. Sang Kil Lee for their guidance.

Especially, I appreciate to Prof. Ki-Chul Hwang for giving me an opportunity to study in a good environment throughout the PhD course. And I express my gratitude to Prof. Seahyoung Lee for his advice and help to complete my dissertation. Also, I must thank Prof. Jong-Chul Park who helped me to get through problems. Without his help, I could not complete my study in Yonsei University.

In addition, I appreciate to my laboratory members, Prof. Woochul Chang, Prof. Soyeon Lim, Prof. Il-Kwon Kim, Prof. Byeong Wook Song, Prof. Seahyoung Lee, Prof. Sang Woo Kim and Prof. Jung-Won Choi, for their generous support and advice. Also, I thank to the colleague for studying together during the 6 years of the PhD course.

Utmost, I would like to express my sincere thanks to my beloved family by naming them one by one; my generous father Seong Kang Seo, my loving mother Jung Sook Choi, my one and only brother Jung Yeon Seo and his lovely wife Sung Yoon Jang. Without their limitless support, I would have not come this far.

Last but not the least, big thanks to all my friends for their support and love, for giving me strength.

The last 6 years in Yonsei University have been a precious time in my life. Thank you.

December, 2017
Hyang-Hee Seo

TABLE OF CONTENTS

LIST OF FIGURES

LIST OF TABLES

ABSTRACT

Multipoint targeting of TGFβ-Wnt transactivation circuit with microRNA 384-5p for cardiac fibrosis

Hyang-Hee Seo

Department of Medical Science
The Graduate School, Yonsei University

(Directed by Professor Jong-Chul Park)

Cardiac fibrosis is a common precursor to ventricular dysfunction and eventual heart failure, and cardiac fibrosis begins with cardiac fibroblast activation. Here, I have demonstrated that the TGF-β signaling pathway and Wnt signaling pathway formed a transactivation circuit during cardiac fibroblast activation and that multipoint targeting of the circuit with miR-384-5p suppressed cardiac fibrosis. TGF-β activated an autopositive feedback loop by increasing Wnt production in cardiac fibroblasts, and Wnt neutralizing antibodies disrupted the feedback loop. A microRNA that simultaneously targeted key receptors of the TGF-β/Wnt transactivation circuit, which I identified as miR-384-5p, significantly attenuated TGF-β-induced cardiac fibroblast activation and ischemia-reperfusion-induced cardiac fibrosis. A

small molecule that prevented pro-fibrogenic stimulus-induced downregulation of endogenous miR-384-5p also significantly suppressed cardiac fibroblast activation and cardiac fibrosis. Thus, modulating a key endogenous miRNA targeting multiple components of the TGF-β/Wnt transactivation circuit can be an effective means to control cardiac fibrosis and has great therapeutic potential.

Key words: microRNA-384-5p, cardiac fibrosis, small molecule

Multipoint targeting of TGFβ-Wnt transactivation circuit with microRNA 384-5p for cardiac fibrosis

Hyang-Hee Seo

Department of Medical Science
The Graduate School, Yonsei University

(Directed by Professor Jong-Chul Park)

I. INTRODUCTION

Cardiac diseases inflicting myocardial tissue damage induces fibrosis of the heart called cardiac fibrosis. Although cardiac fibrosis initially occurs as a compensatory response to maintain the structural and functional integrity of the damaged heart, when cardiac fibrosis is severe and prolonged, ventricular dysfunction and, ultimately, heart failure can result.[1, 2] Activation of fibroblasts or myofibroblast (myoFB) formation by various cytokines, such as transforming growth factor-β (TGF-β), constitutes an early event in cardiac fibrosis. For example, during the first 0-4 days after cardiac injury, called the inflammatory phase, massive death of cardiomyocytes occurs, causing an inflammatory response, and the expression of TGF-β increases. For the next

3-4 days, called the reparative phase, cytokines, such as TGF-β, activate cardiac fibroblasts (CFs), which trigger deposition of the fibrogenic extracellular matrix.[3] In adult mammals, the fibrotic scar that forms in the damaged heart is permanent and further promotes reactive fibrosis, which increases myocardial stiffness and reduces compliance.[2] Therefore, prevention of CF activation can be an effective means to control pathological cardiac fibrosis, and a deeper understanding of the activation mechanism can provide critical information to develop an optimized therapeutic strategy for cardiac fibrosis.

Regarding the activation of CFs, both the TGF-β pathway[4-6] and Wnt signaling pathway[7] significantly contribute to cardiac fibrosis, and a possible interaction between these two pro-fibrogenic pathways has been suggested. Previous studies have reported that TGF-β-induced skin fibrosis requires Wnt signaling activation[7] and that Wnt3a induces myoFB differentiation of mouse embryonic fibroblasts in a TGF-β and β-catenin-dependent manner.[8] Furthermore, a very recent study demonstrated that TGF-β controls myoFB formation via Wnt secretion in autoimmune myocarditis.[9] These studies strongly imply the existence of a TGF-β/Wnt transactivation circuit that functions in fibrosis. Therefore, a careful examination of the mechanisms that underlie such a pro-fibrogenic transactivation circuit may provide critical information for developing a therapeutic strategy to disrupt the circuit and

subsequently prevent cardiac fibrosis and heart failure.

MicroRNAs (miRNAs) negatively regulate the expression of their target genes at post-transcriptional level.[10] Presumably, thousands of miRNAs regulate approximately 30% of all coding genes in humans, affecting virtually every aspect of numerous biological processes.[11-13] Therefore, miRNAs may also contribute to the initiation and maintenance of the TGF-β/Wnt transactivation circuit, if the circuit exists. Considering that a single miRNA can target multiple genes simultaneously,[14] a key miRNA that affects both signaling pathways may exist. In this study, as a proof of concept, I hypothesized that the formation and maintenance of a TGF-β/Wnt transactivation circuit involves a key miRNA-mediated mechanism and that modulating the expression of this miRNA will disrupt the circuit, preventing progression of cardiac fibrosis

II. MATERIALS AND METHODS

1. Isolation of neonatal rat cardiac fibroblasts

The hearts of 8week-old Sprague Dawley rat pups were used for the study. The extracted ventricle was washed with Dulbecco's phosphate-buffered saline (DPBS) solution, pH 7.4 without Ca^{2+} and Mg^{2+} (Thermo Fisher Scientific, MA, USA). Using micro-dissecting scissors, hearts were minced to pieces of approximately 1 mm^3 in size and treated with 10 ml of collagenase II (0.8 mg/ml, 262 units/mg, Worthington, OH, USA) for 5 minutes at room temperature. The initial supernatant was discarded by decantation and the remained tissues were treated with fresh collagenase II solution for an additional 5 minutes at 37 °C. The supernatant containing cells was transferred to a tube containing cell culture medium (DMEM/F-12 containing 10% fetal bovine serum, Thermo Fisher Scientific) and centrifuged at 1,200 rpm for 4 minutes at room temperature. The cell pellets were re-suspended in 5 ml of cell culture medium. The above procedures were repeated 7−9 times until little tissues were left. The cell suspensions were collected and incubated in 100 mm tissue culture dishes for 30 minutes for attachment. Unattached cells were discarded by changing culture medium. Attached fibroblasts were then cultured with DMEM/F-12 containing 10% (v/v) FBS in a CO_2 incubator at 37°C. Cardiac fibroblasts with passages between 1 and 3 were used for all studies.

2. MicroRNA transfection

MicroRNAs and scrambled RNA oligomer (negative control scrambled miRNA, N.C.) were purchased from Genolution Inc. (Seoul, Korea). Transfection of microRNAs was performed using a TransIT-X2 system (Mirus Bio LLC, Madison, WI, USA). Briefly, cells were seeded at a density of 7×10^5 cells per 60 mm culture plates. The TransIT-X2 reagent was diluted with Opti-MEM and combined with microRNA mimics. The mixture was added to each well. After 24 hours of incubation in a CO_2 incubator at 37°C, the medium was changed to fresh 10% FBS DMEM.

3. Conventional polymerase chain reaction

Total RNA was extracted using TRIzol (Sigma-Aldrich, MO, USA, 500 μL per 60 mm culture dish). Chloroform (100 μL) was added to the extract and each sample was vortexed for 15 seconds. The mixtures were centrifuged at 12,000rpm for 15 minutes at 4°C, and the transparent upper layer was collected in a new tube. Each sample was mixed with 300 μL of isopropanol. The samples were centrifuged at 12,000rpm for 10 minutes at 4°C. The supernatant was discarded and the pellet was washed using 75% (v/v) ethanol. The samples were centrifuged at 12,000rpm for 5 minutes at 4°C, and the supernatant was discarded. The pellet was air-dried at room temperature, and dissolved in 20 μL of nuclease-free water. Complementary DNA (cDNA) was

generated using 500 ng of total RNA with AccuPower PT PreMix (Bioneer, Seoul, Korea) according to the manufacturer's instructions. The PCR conditions consisted of denaturing at 94°C for 3min, followed by 25 cycles of denaturation at 94°C for 30 seconds, annealing at 55°C for 30 seconds, and extension at 72°C for 30 seconds, before a final extension at 72°C for 10 minutes. PCR products were separated by electrophoresis in 1.2% (w/v) agarose gels (Bio-Rad, CA, USA). Glyceraldehyde-3-phosphate dehydrogenase (Gapdh) was used as an internal standard.

4. Quantitative real-time polymerase chain reaction (Real-time PCR)

Total RNA extraction procedure was identical to that of RT-PCR. cDNA was generated using 10 ng of purified total RNA with Taqman® MicroRNA Reverse Transcriptase Kit (Applied Biosystems, CA, USA) in combination with Taqman® MicroRNA Assays. For normalization, U6 control transcripts were used. Amplification and detection of specific products were performed in a Step One plus Real-Time PCR system (Applied Biosystems) at 95°C for 10 minutes, followed by 40 cycles of 95°C for 15 seconds and 60°C for 60 seconds.

5. Luciferase reporter assay

The 3'UTR fragment of Fzd-1, Fzd-1, TGFβR1 and LRP6 (covering 50 bp upstream and 50 bp downstream of the miR-384-5p binding sequence) was

used for luciferase assay. Approximately 120 bp-long 3' UTR fragment of each target was PCR amplified by using primers containing XhoI (forward) and SalI (Reverse) enzyme site. The PCR product was then cloned into pmirGLO Dual Luciferase vector (Promega, WI, USA) using the XhoI and SalI enzyme site. For transfection, Hela cells were seeded in 24 well plate at a density of 5 x 10^4 cells/well. When the cells reached confluency of near 80 %, 500 ng of pmirGLO vectors containing the 3'UTR fragment was transfected by using lipofectamin LTX system (Thermo Fisher Scientific) according to the manufacturer's instruction. Twenty four hours after the transfection, luciferase activity was measured using Dual-luciferase reporter assay system (Promega). The Renilla luciferase was used to normalize the cell number and the transfection efficiency.

6. Promoter assay

The promoter region of rno-miR-384-5p (miRBase, MIMAT0005309) from -1 up to -3000 was amplified using KpnI site containing forward primers containing set of 5'-AAG GTA CCA TAG ATC TGT AAT AAC TC-3' (1,000 bp fragment, F1), 5'-AAG GTA CCT TCT CAG CTA ACC AGC TC-3' (1,250 bp fragment, F2), 5'-AAG GTA CCG AGA GCA GTG TAG AGC TC-3' (1,500 bp fragment, F3), 5'-AAG GTA CCA AGA GAG TGT ATA CCA T-3' (1,750 bp fragment, F4), 5'-AAG GTA CCG TAT GTT TAG CTT TCT TT-3' (2,000 bp fragment, F5), and 5'-AAG GTA CCG GTA CTC TTC

ATT TCT TT-3' (3,000 bp fragment, F6). For XhoI site containing reverse primer, 5'- AAC TCG AGT AAC ATT TCG CTG CAA CA-3' was used. PCR amplicons were digested with KpnI and XhoI, and inserted into the pGL3-basic vector (Promega, Madison, WI, USA). For transfection, Hela cells were seeded in 24 well plate at a density of 5 x 10^4 cells/well. When the cells reached confluency of near 80 %, 500 ng of pGL3 vectors containing the promoter fragment was transfected by using lipofectamin LTX system (Thermo Fisher Scientific) according to the manufacturer's recommendation. Twenty four hours after the transfection, luciferase activity was measured.

7. Western blot

The cells were washed in PBS and lysed in lysis buffer (Cell Signal Technology, MA, USA). Protein concentrations were determined using the BCA Protein Assay Kit (Thermo Fisher Scientific). Equal amount of proteins were separated in a sodium dodecyl sulfate-polyacrylamide gel (SDS-PAGE) and transferred to a polyvinylidene difluoride membrane (Millipore, Billerica, MA, USA). After blocking the membrane by using Tris-buffered saline-Tween 20 (TBS-T, 0.05% Tween 20) and 10% skim milk for 1 hour at room temperature, the membranes were incubated with appropriate primary antibodies. Antibodies specific to α-SMA and β-actin were purchased from Abcam (Cambridge, UK), and the following antibodies were purchased from Cell Signaling Technology : Collagen type I, p-JNK, JNK, p-GSK-3β,

GSK-3β, p-P65, P65, p-P38, p38, p-IKKα, Fzd1, LRP6, p-Smad and Smad. Antibodies specific to Collagen type III, p-CamK IIα, CamK II, β-catenin, p-TAK1, Wnt3a, TGF-β, and TGFβR1 were from Santa Cruz Biotechnology (TX, USA). Additionally, antibodies specific to Lamin B2 (Thermo Fisher Scientific) and Fzd-2 (OriGene, MD, USA) were also used. After incubation with appropriate antibodies overnight at 4°C, the membrane was washed three times with 0.05% TBS-T for 10 minutes each and then incubated for 1 hour at room temperature with horseradish peroxidase-conjugated secondary antibodies. The immune-positive bands were detected by an enhanced chemiluminescence (ECL) reagent (Santa Cruz Biotechnology,). The band intensities were quantified using NIH Image J version 1.34e software.

8. Nuclear and cytosolic fractionation

For nuclear and cytoplasmic extraction, NE-PER Nuclear and Cytoplasmic Extraction Reagents (Thermo Fisher Scientific) were used according to the user manual provided by the manufacturer.

9. Immunocytochemistry

CFs were cultured in four-well slide chambers at a density of $2.2x10^4$. The cells were permeabilized using 0.1% Triton X-100 for 10 min. Next, the cells were blocked for 1 hour in a blocking solution (2% bovine serum albumin and 10% horse serum in PBS) and incubated with α-SMA (Abcam,

Cambridge, UK), Vimentin (Abcam), vWf (Santa Cruz Biotechnology), P65 (Cell Signaling Technology) and β-catenin antibodies (Santa Cruz Biotechnology). FITC-conjugated mouse and rabbit secondary antibodies (Jackson ImmunoResearch Laboratories, West Grove, PA, USA) were used. Immunofluorescence was detected by a confocal microscope (LSM710; Carl Zeiss Microscopy GmbH, Jena, Germany).

10. Wound healing assay

CFs were plated at a density of $2.5x10^5$ cells/well in six-well plates. When the cells reached 90% confluence, cells were starved for 12 hours. After starvation, scratches were produced with 200μl pipette tips and images were captured using an Axiovert 40 C inverted microscope (Carl Zeiss Microscopy GmbH) equipped with a Powershot A640 digital camera (Canon, Tokyo, Japan). The medium was replaced with or without small molecule and TGF-β. The migrated area was captured at 0 and 24 hours after TGF-β treatment and the percent of area re-covered by growth was calculated.

11. Transwell migration assay

CFs ($0.6x10^4$cells) were plated in the upper chamber of Transwell assay plates with 8μm filter pore size (Costar Corning, Corning, NY, USA). The cells were incubated in serum deprivation media for 12 hours, and small molecule was added to upper chamber. After 1 hour, TGF-β was added to the

bottom chamber, and incubated at 37°C for 24 hours. After incubation, the migrated cells were stained with 0.25% crystal violet. Non-migrated cell on the inside of the upper chamber were removed with cotton swabs.

12. Collagen gel contraction assay

CFs were transfected miR-384-5p or anti-miR-384-5p at concentration 100 nM and 50 nM, respectively, for 24 hours. After additional 24 hours of incubation in culture media containing 10% FBS, CFs were re-suspended in medium at a density of $3x10^6$ cells/ml. Subsequently, 100 μl cell suspension was mixed with 400 μl collagen solution (Sigma-Aldrich, St Louis, MO, USA) and 1M NaOH. Five hundred μl of cell suspension containing collagen was caste into 24-well cell culture plates and incubated at 37°C for 1 hour for polymerization. After 1 hour, 600 μl of DMEM was added to each well, and gels were released from the surface of the plate by using a pipette tip. Drug 145 was pretreated for 1 hour and TGF-β1 (5ng/ml) was added.

13. Cell proliferation assay

For determining cell proliferation, WST-8 (2-(2-methoxy-4-nitrophenyl)-3-(4-nitrophenyl)-5-(2,4-disulfophenyl)-*2H*-tetrazolium, monosodium salt solution) (cell counting kit, CCK-8, Dojindo Molecular Technologies, Inc., Kumamoto, Japan) was added to each well (10% (v/v)) and incubated at 37°C

for 2 hours to allow formation of WST-8 formazan. The absorbance of a water soluble formazan dye was measured at 450 nm using a microplate reader (Molecular Devices, CA, USA).

14. Antibody neutralization assay

CFs ($2.2x10^5$ cells) were plated into 6well culture plates. Wnt3a-neutralizing antibodies or IgG control antibodies (15 ug/ml, each) were added to appropriate wells 1 hour prior to TGF-β treatment. After 24 hours of TGF-β treatment, cells were lysed for western blot analysis.

15. Detection of miR-384-5p using molecular beacon

Molecular beacons for detecting miR-384-5p were prepared by annealing Cy3-modified long sequence (Cy3-ACATTTATTAAGGATCCGTTACA) and black hole quencher (BHQ1) modified short sequence (BHQ1-TGTAAATAAT). After seeding CFs in 96 well culture plates, the cells were treated with 10 μM of D145 or transfected with increasing concentrations of miR-394-5p (10, 20, and 50 nM) for 48 hours. To detect miR-384-5p, molecular beacons were delivered to CFs at a concentration of 50 nM using a lipofectamin LTX system. After 24 hours after the molecular beacon delivery, Cy3 fluorescence was detected by using a confocal microscope (LSM710; Carl Zeiss Microscopy GmbH, Jena, Germany).

16. Rat cardiac ischemia/reperfusion (I/R) injury model

All experimental procedures for animal studies were approved by the Committee for the Care and Use of Laboratory Animals, Yonsei University College of Medicine, and performed in accordance with the Committee's Guidelines and Regulations for Animal Care. I/R-injury was produced in male Sprague-Dawley rats (200 ± 50 g) by surgical occlusion of the left anterior descending coronary artery. Briefly, after induction of anesthesia with zoletil (0.8 ml/kg) and rompun (0.2 ml/kg), the rats were intubated, and ventilation (62 strokes/min, tidal volume 8-10 ml/kg) was maintained using a Harvard ventilator (MA, USA). After intubation, the third and fourth ribs were cut to open the chest, and the heart was exteriorized through the intercostal space. The left coronary artery was then ligated 2–3 mm from its origin with a 6-0 prolene suture (Ethicon, NJ, USA). Reperfusion was conducted after 1 hour of ischemia. For transplantation, microRNA (10 μg/head) and reagent mixture were prepared in 60 μl and injected from the injured region to the border using a Hamilton syringe (Hamilton Co., NV, USA) with a 30 gauge needle. For drug injection, D145 was intravenously (i.v.) injected right after I/R-injury at concentration of 10 μM (whole blood volume of an individual rat was approximated as 7% of body weight). Throughout the operation, animals were ventilated with 95% O_2 and 5% CO_2 using a Harvard ventilator (Holliston, MA, USA). For each group, 5 animals (ligation, miR-384-5p injection, Drug 145 injection, DMSO injection and Reagent injection) were

used. Animals were sacrificed 1 to 2 weeks after the surgery for analysis, depending on experiments conducted.

17. Statistical analysis

Quantitative data were expressed as the means ± S.D. of at least 3 independent experiments. For statistical analysis, one-way ANOVA with Bonferroni correction was performed using OriginPro 8 SR4 software (ver. 8.0951, OriginLab Corporation, MA, USA) if there were more than 3 groups. A p value of less than 0.05 was considered statistically significant.

III. RESULTS

1. Characterization of primary cultured CFs

A. Cell type specific marker expression of cultured CFs

TGF-β is a well-established cytokine known to induce activation of CF.[15] For the *in vitro* model of TGF-β-induced CF activation used in the present study, primary cultured CFs between passages 1 and 2 were used. To characterize the primary cultured CFs and to confirm that the primary CFs maintained an inactivated status in the absence of stimulation, the cells were immunostained with von Willebrand factor (vWF, an endothelial cell marker),[16] α-smooth muscle actin (α-SMA), a hallmark of mature myofibroblasts (myoFBs),[17] and vimentin, a common fibroblast marker.[18] The cultured primary CFs were negative for both vWF and α-SMA, but positive for vimentin (Fig. 1). This indicated that the primary cultured CFs had characteristics of CFs and remained inactivated without stimulus.

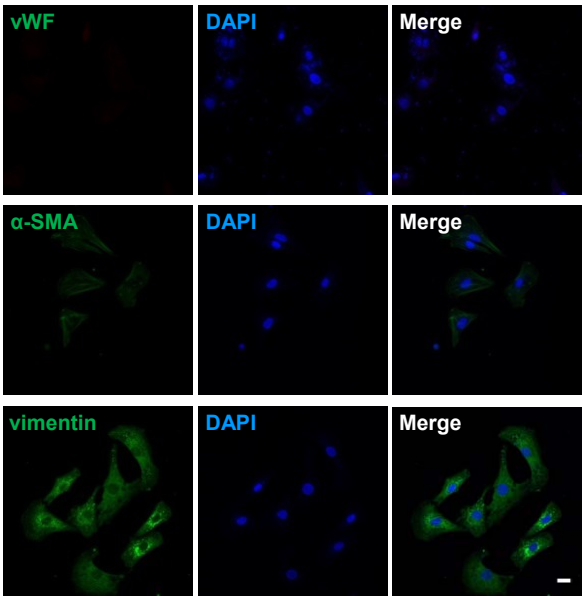

Figure 1. Characterization of cultured primary cardiac fibroblast (CFs). Primary CFs were immunostained with von Willebrand factor (vWF, an endothelial cell marker), α-smooth muscle actin (α-SMA, a myofibroblasts marker), and vimentin, a fibroblast marker. The nuclei were stained with DAPI (blue). Scale bar = 20 μm.

2. Effects of TGF-β on CFs activation

A. TGF-β induces α-SMA expression of CFs.

CFs were serum-starved for 12 hours and treated with increasing concentration of TGF-β (1, 5, and 10 ng/ml) for 48 hours. The expression levels of α-SMA were examined by western blotting to verify the effect of TGF-β on CF activation. The expression levels of α-SMA were significantly increased by TGF-β at a concentration of 1 ng/ml or higher (Fig. 2A). The TGF-β-induced increase in α-SMA expression was also confirmed by immunocytochemical staining (Fig. 2B).

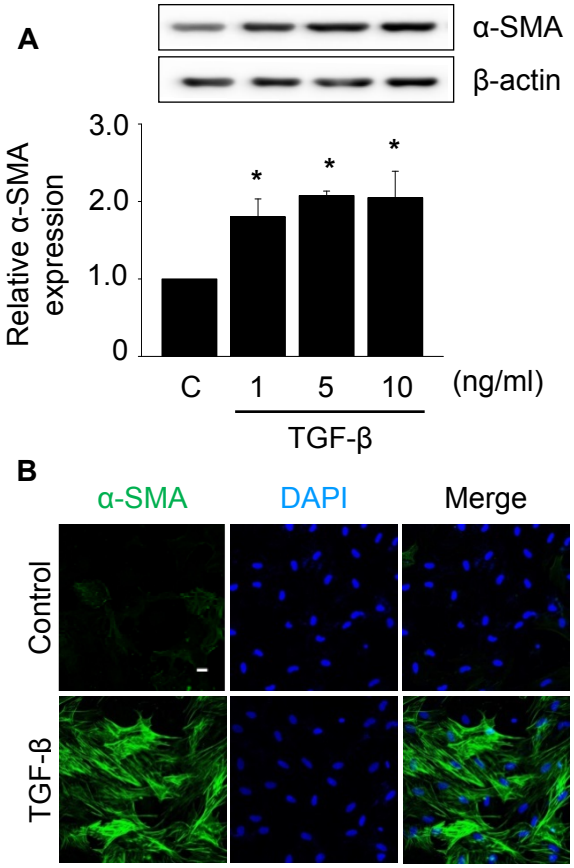

Figure 2. Effect of TGF-β on the expression of α-SMA in primary CFs. Primary CFs were plated at a density of $2.5x10^4$ cells/well in 4-well plates. After 24hr, CFs were serum-starved for 24 hours. (A) After starvation, CFs were treated with TGF-β for 24 hours at concentrations as indicated in serum-free DMEM. The expression level of α-SMA was analyzed by western blotting. The expression level of α-SMA was normalized to the expression level of β-actin. C: untreated control. Quantitative data were expressed as the means ± S.D. The similar results were obtained in at least 3 independent experiments. *$p < 0.05$ compared to untreated control. (B) After starvation, CFs were treated with 5 ng/ml of TGF-β for additional 24

hours. The expression of α-SMA was examined by immunocytochemical staining. The nuclei were stained with DAPI. Scale bar represents 20 μm.

B. TGF-β increases collagen production in CFs

The effect of TGF-β on collagen production, which is known to be increased in activated CFs or myoFBs,[19] was examined. According to the data, 5 ng/ml TGF-β significantly increased the production of collagen type I and III at both the mRNA (Fig. 3A) and protein level (Fig. 3B).

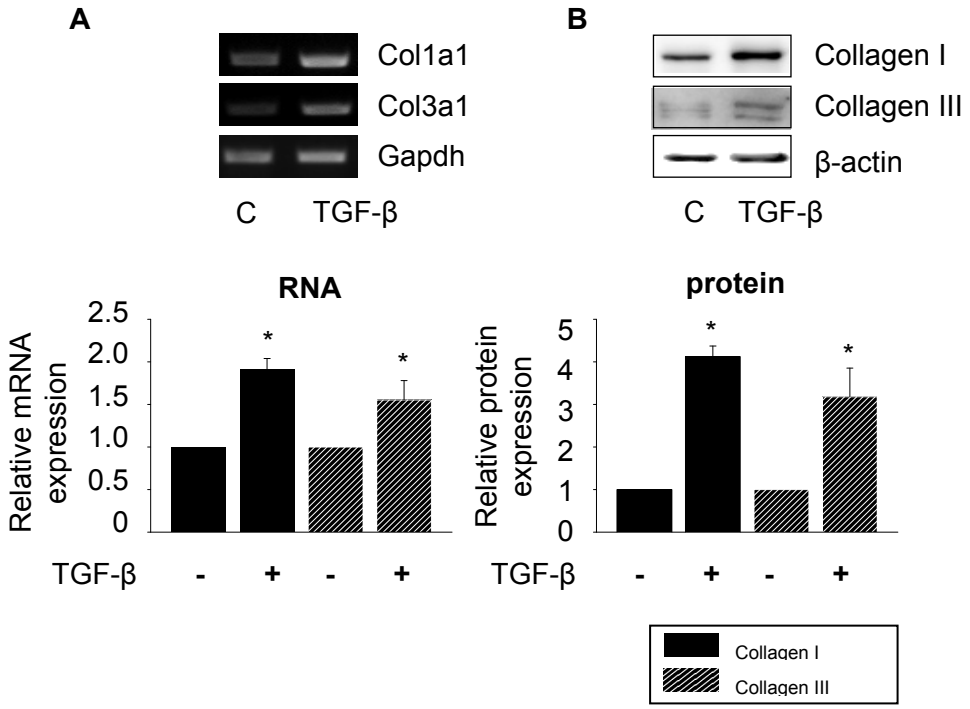

Figure 3. TGF-β-induced expression of collagen type I and III in primary CF. Primary CFs were serum-starved for 24 hours, and then treated with 5 ng/ml of TGF-β for an additional 24 hours. (A) The mRNA expression of collagen I and III was examined by conventional PCR. C: control. Quantitative data were expressed as the means ± S.D. of at least 3 independent experiments. **p* <0.05. (B) The expression of collagen I and III was examined by western blotting. Quantitative data were expressed as the means ± S.E.M. The similar results were obtained in at least 3 independent experiments. **p* <0.05.

C. TGF-β increases contractility of CFs

Collagen gel contraction analysis was performed to examine the effect of TGF-β on collagen contractility, a characteristic of activated fibroblasts.[20] TGF-β significantly decreased the size of the collagen gel matrix indicating the increased collagen contractility of the CFs (Fig. 4). These data indicated that our *in vitro* model of TGF-β-mediated activation of CF worked properly.

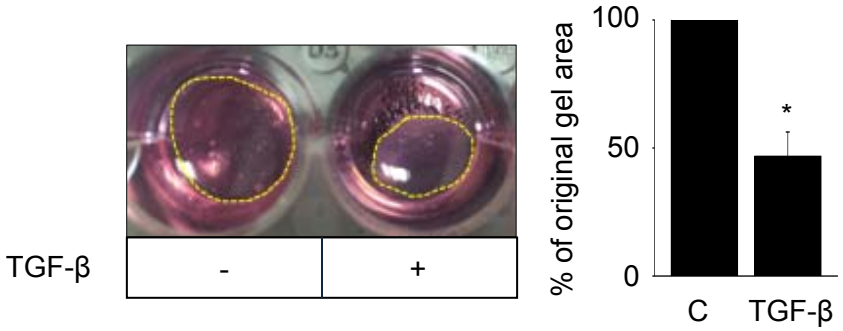

Figure 4. TGF-β increases collagen contractility of CFs. CF-containing collagen gels were serum-starved for 12 hours. After starvation, gels were stimulated with TGF-β (5 ng/ml) for 48 hours and photographed at 48 hour. The sizes of the gels were measured and analyzed. Quantitative data were expressed as the means ± S.E.M. The similar results were obtained in at least 3 independent experiments. *p <0.05 compared to the TGF-β-untreated control.

3. TGF-β-induced Wnt signaling activation in CFs.

A. TGF-β activates canonical Wnt signaling pathway in CFs.

The Wnt signaling pathway can be divided into 3 sub-pathways: the canonical, planar cell polarity, and Wnt/Ca^{2+} pathway.[21] c-Jun N-terminal kinase (JNK) and Ca^{2+}/calmodulin-dependent protein kinase II (CamKII) mediate planar cell polarity pathway and Wnt/Ca^{2+} pathway, respectively.[22, 23]

According to the data, TGF-β did not increase the expression of the phosphorylated forms of either CamKII or JNK, indicating that neither the Wnt/Ca^{2+} pathway nor the planar cell polarity pathway was activated by the TGF-β treatment in our *in vitro* system. However, the expression levels of cytoplasmic -β-catenin (β-catenin) and phosphorylated glycogen synthase kinase 3 -β (p-GSK3β^{ser9}), which are representative markers of canonical Wnt signaling activation,[24] were increased by TGF-β (Fig. 5).

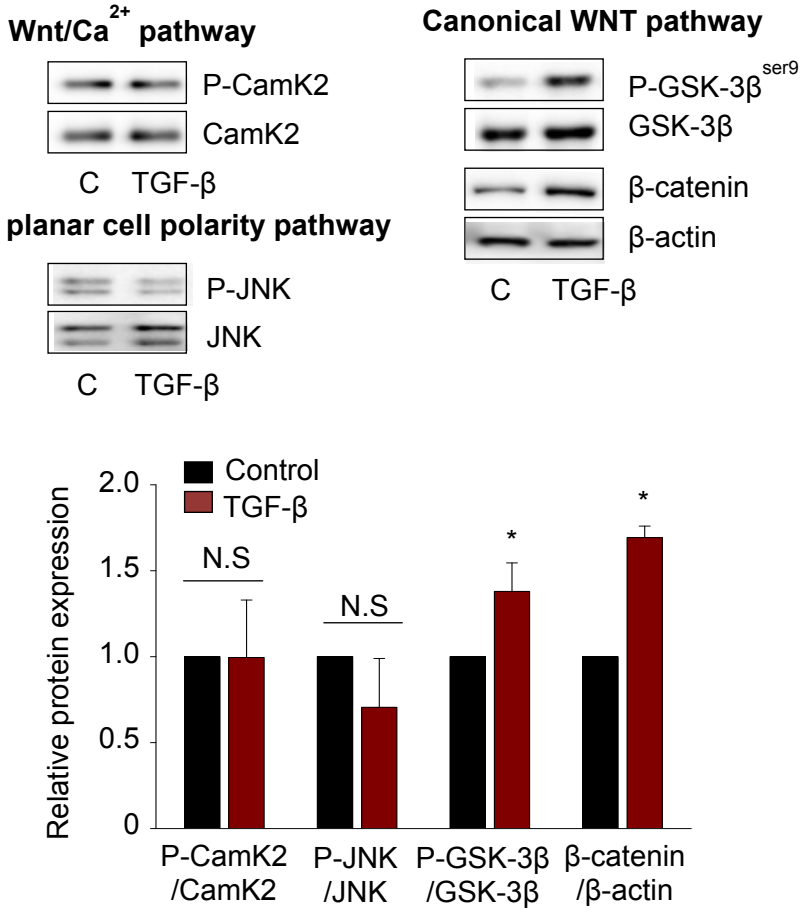

Figure 5. TGF-β-induced activation of canonical Wnt signaling pathway in CFs. Serum-starved CFs were treated with 5 ng/ml TGF-β for 30 minutes, and the expression levels of the markers of the planar cell polarity pathway, Wnt/Ca2+ pathway, and canonical pathway were detected by western blotting. Quantitative data were expressed as the means ± S.E.M. The similar results were obtained in at least 3 independent experiments. **p* <0.05 compared to the TGF-β-untreated control.

B. TGF-β increases nuclear translocation of β-catenin in CFs.

Since nuclear translocation of β-catenin is a hallmark of activated canonical Wnt signaling,[24] the expression of nuclear β-catenin was examined. TGF-β significantly increased nuclear translocation of β-catenin (Fig. 6), and this observation confirmed that TGF-β stimulated activation of canonical Wnt signaling in primary CFs at the given concentration.

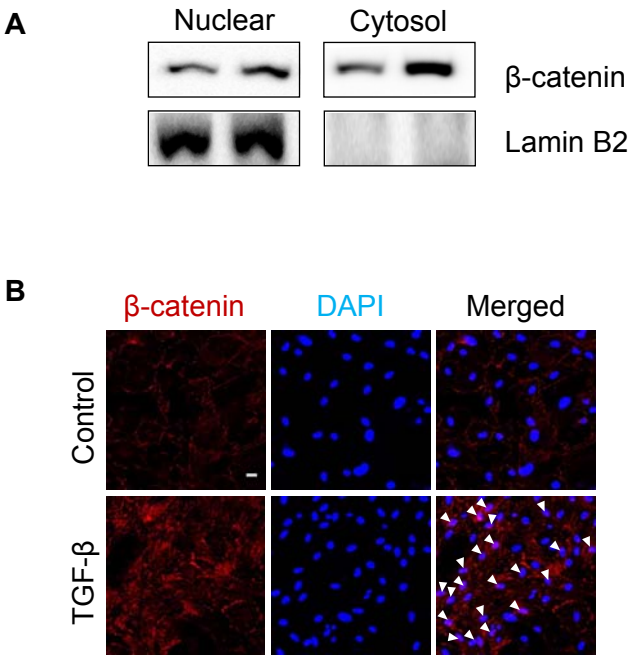

Figure 6. Nuclear translocation of β-catenin in TGF-β treated CFs. (A) Serum-starved CFs were treated with 5 ng/ml TGF-β for 30 minutes, and cytosolic and nuclear expression of β-catenin was detected by western blotting. Lamin B2 was used as an internal control for the nuclear fraction. (B) Immunocytochemical staining of β-catenin. Nuclei were stained with DAPI. White arrows indicate nuclear localization of β-catenin. Scale bar represents 20 μm.

4. Effect of fibrogenic stimuli on the expression of Wnt ligands and related receptors

A. Effect of ischemia/reperfusion (I/R) and TGF-β on the expression of Wnt ligands and related receptors.

Wnt signaling is initiated by combinatorial interactions between 19 different Wnt ligands[25] and 10 different related receptors known as Fzds.[26] Previous studies have reported that Fzd1 and Fzd2 were upregulated in cardiac myoFBs[27] and that inhibition of the interaction between Wnt3a/Wnt5a and their putative receptors Fzd1/Fzd2 prevented heart failure after myocardial infraction (MI)[28]. In this study, the mRNA expression levels of Fzd1, Fzd2, Wnt3a, and Wnt5a was significantly increased in the I/R-injured heart tissue compared to levels in the normal control (Fig. 7). In the TGF-β-treated primary CFs, the mRNA expression levels of Fzd1 and Fzd2 was significantly increased at 12 hours (Fig. 8A, left panel). Wnt3a mRNA expression was significantly increased by TGF-β at 1 hour and thereafter, for up to 12 hours. However, TGF-β had no significant effect on Wnt5a mRNA expression in TGF-β-treated primary CFs (Fig. 8B, right panel). These data suggest that, between Wnt3a and Wnt5a, Wnt3a may be more relevant to cytokine-induced activation of CFs and that the observed increase in Wnt5a in the I/R-injured heart may be due to cardiac cells other than CFs.

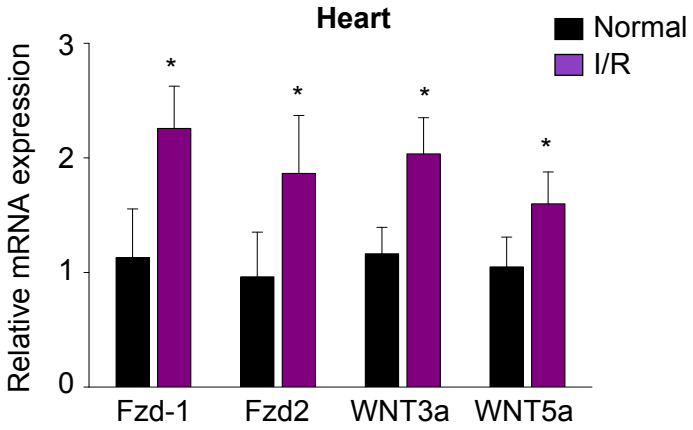

Figure 7. The effect of I/R on the expression of Wnt ligands and related receptors. The mRNA expression levels of Fzd1, Fzd2, Wnt3a, and Wnt5a in the I/R-injured heart was examined by semi-quantitative PCR. The I/R-injury samples were collected 7 days after the injury. Normal heart (Normal) sample was used as a control. Quantitative data were expressed as the means ± S.E.M. The similar results were obtained in at least 3 independent experiments. *p <0.05 compared to the normal control.

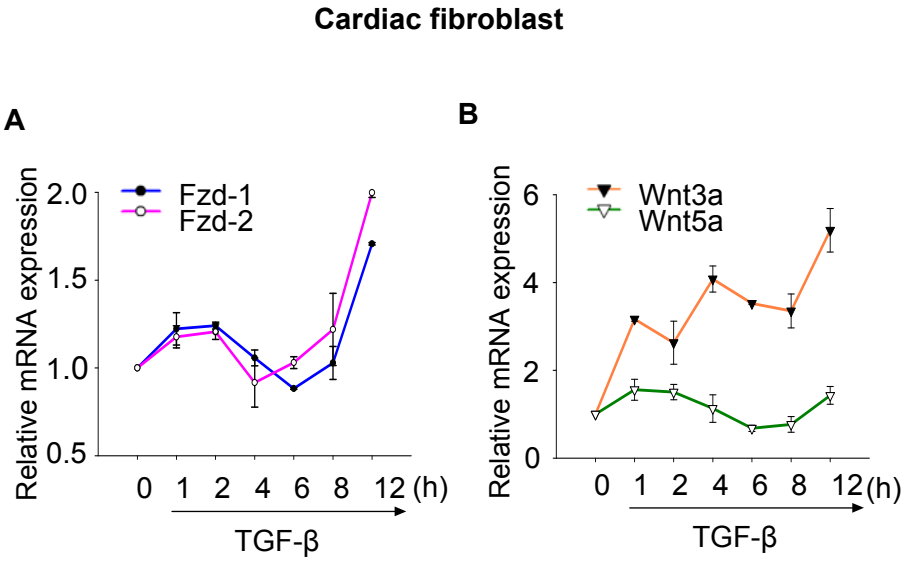

Figure 8. Effect of TGF-β on the expression of Wnt ligands and related receptors. The mRNA expression levels of (A) Fzd1, Fzd2, (B) Wnt3a, and Wnt5a in the TGF-β-treated primary CFs. The cells were treated with 5 ng/ml TGF-β for up to 12 hours as indicated. Untreated CFs were used as a control. Quantitative data were expressed as the means ± S.E.M. The similar results were obtained in at least 3 independent experiments. **p* <0.05 compared to the control.

5. Wnt3a mediates TGF-β-induced activation of autopositive feedback via NF-κB in primary CFs

A. TGF-β activates NF-kB pathway

A recent study has reported that TGF-β induces the expression of Wnt proteins via the TGF-β-activated kinase 1 (TAK1) pathway.[9] TGF-β signaling can be divided into the Smad and non-Smad pathways, and the TAK1 pathway is a non-Smad pathway.[29] TGF-β-induced TAK1 activation can subsequently lead to activation of nuclear factor kappa-light-chain-enhancer of activated B cells (NF-kB), JNK, or P38.[30] As shown in Fig. 9, the expression of phosphorylated JNK and p38 was not affected by the TGF-β treatment, whareas the expression of phosphorylated P65 (p-P65), a main subunit of NF-kB,[31] significantly increased. This observation indicates that the TGF-β-induced production of Wnt3a might be NF-**κ**B-dependent.

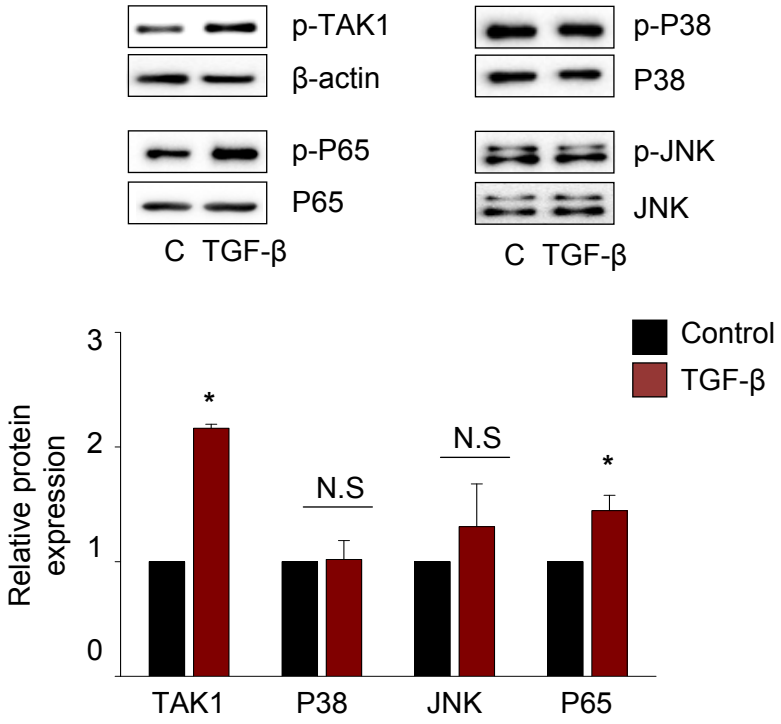

Figure 9. TGF-β activates TAK1-P65 signaling axis in treated CFs. The cells were treated with 5 ng/ml TGF-β for 30 min, and the activation (phosphorylation) statuses of the signaling molecules TAK1were evaluated. Untreated CFs were used as a control. Quantitative data were expressed as the means ± S.E.M. The similar results were obtained in at least 3 independent experiments. *p <0.05 compared to the control.

B. TGF-β increases the expression of Wnt3a in a NF-κB-dependent way

Pretreatment with caffeic acid phenethyl ester (CAPE), a potent inhibitor of NF-kB (Fig. 10),[32] significantly decreased the expression of both p-P65 and Wnt3a (Fig. 11), indicating that TGF-β-induced Wnt3a expression was mediated by NF-κB. A previous study reported that Wnt3a increased the expression of TGF-β in mouse embryonic fibroblast.[8] Therefore, I speculated that the increased Wnt3a production by TGF-β in the present study would, in turn, further enhance the expression of TGF-β, creating an auto-positive feedback loop.

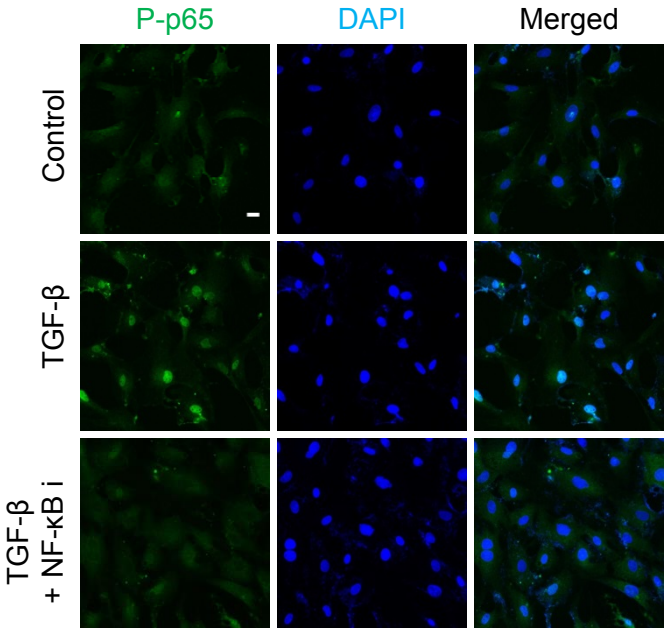

Figure 10. Effects of NF-κB inhibitor on P65 activation. The cells were plated in 4well plate at a density of $2.5x10^4$ cells /well. Cells were starved for 12 hours and treated NF-κB inhibitor CAPE (NF-κB i, 5 ng/ml) for 30 minutes prior to 2 hours of TGF-β (5 ng/ml) in serum free DMEM. Nuclei were stained with DAPI. Scale bar represents 20 μm.

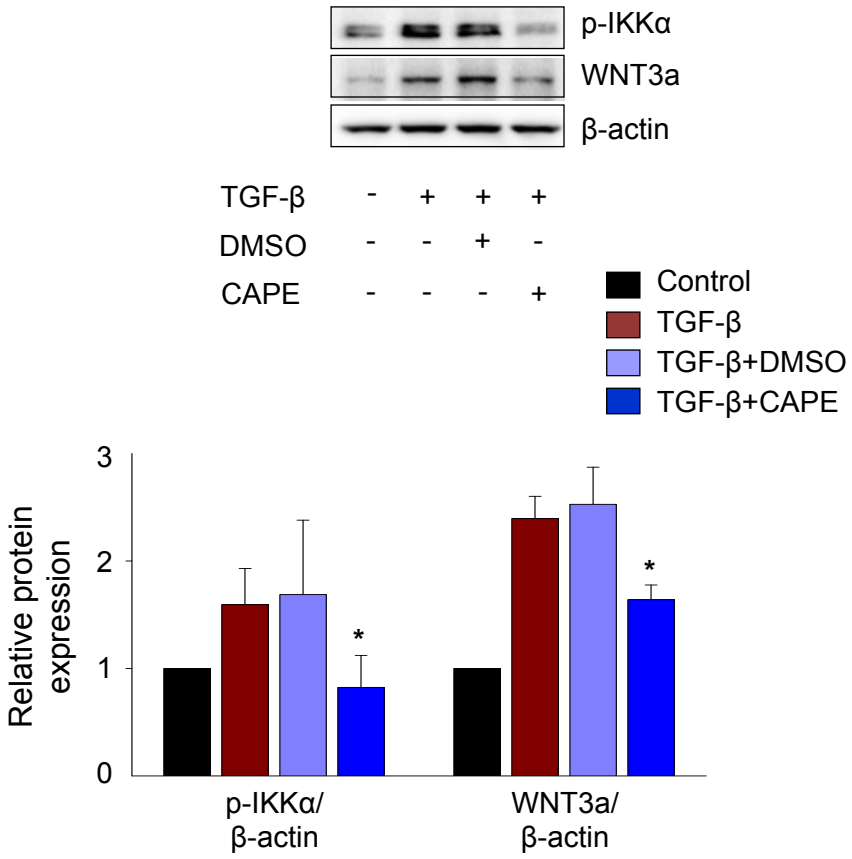

Figure 11. Effects of a NF-κB inhibitor on Wnt3a expression. The cells serum starved for 12 hours. After starvation, cells were treated with 5 ng/ml CAPE for 30 minutes, and then further exposed to TGF-β (5 ng/ml) for 2 hours in serum free media. The expression levels of phosphorylated IKKα (p-IKKα) and Wnt3a were examined by western blotting. IKKα: Inhibitor of kappa B kinase. Untreated CFs were used as a control. Quantitative data were expressed as the means ± S.E.M. The similar results were obtained in at least 3 independent experiments. **p* <0.05 compared to the TGF-β-treated control.

C. Wnt3a increased the expression of TGF-β

As shown in Figure 12, Wnt3a significantly increased the expression of both β-catenin and TGF-β. Furthermore, TGF-β significantly increased the mRNA expression of TGF-β itself in a time-dependent manner for up to 4 hours (Fig. 13). These data strongly suggested that TGF-β activated an auto-positive feedback loop which may be mediated by Wnt3a.

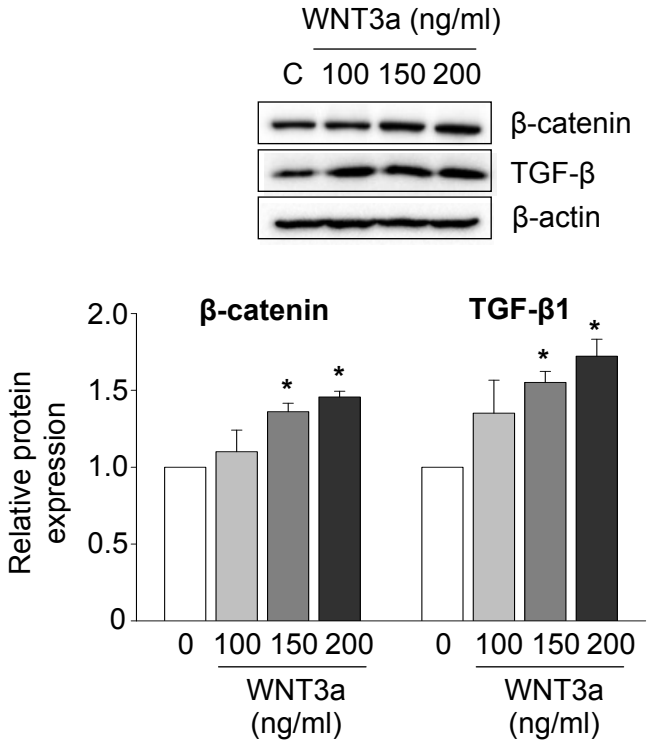

Figure 12. Effects of WNT3a on TGF-β expression. The cells were starved for 12 hours. After starvation, cells were treated with increasing concentrations of human recombinant WNT3a for 4 hours as indicated, and the expression levels of β-catenin and TGF-β were examined by Western blotting. Quantitative data were expressed as the means ± S.E.M. The similar results were obtained in at least 3 independent experiments. **p* <0.05 compared to the untreated control.

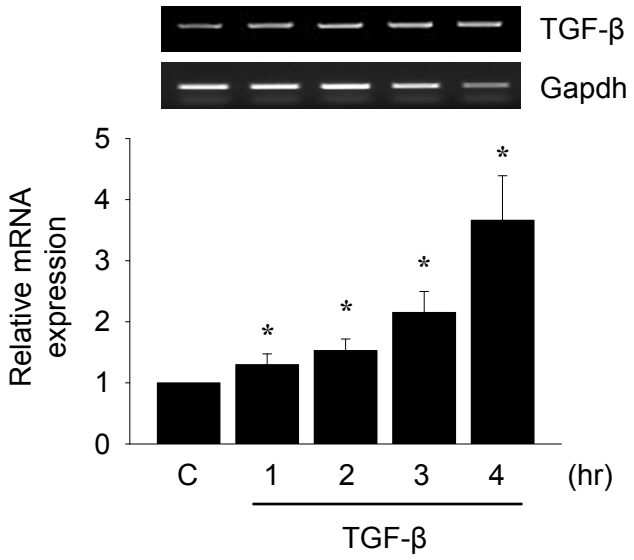

Figure 13. Time-dependent expression of TGF-β in TGF-β treated CFs. The cells were treated with TGF-β (5 ng/ml) for up to 4 hours, and the mRNA expression levels of TGF-β were examined by conventional-PCR. Quantitative data were expressed as the means ± S.E.M. The similar results were obtained in at least 3 independent experiments. **p* <0.05 compared to the untreated control.

D. Wnt3a neutralizing antibody suppresses both Wnt signaling activation and CF activation.

Wnt3a neutralizing antibodies significantly attenuated the expression of β-catenin and p-GSK3β^{ser9}, and also significantly suppressed TGF-β and collagen type I expression in TGF-β-treated CFs (Fig. 14). Furthermore, pretreatment with CAPE and FH535, a Wnt/β-catenin signaling inhibitor,[33] significantly suppressed the production of TGF-β (Fig. 15). These data indicate that TGF-β induces production of Wnt3a, and that in turn, the increased Wnt3a further increases TGF-β production, establishing a transactivation circuit between TGF-β signaling and Wnt signaling in primary CFs.

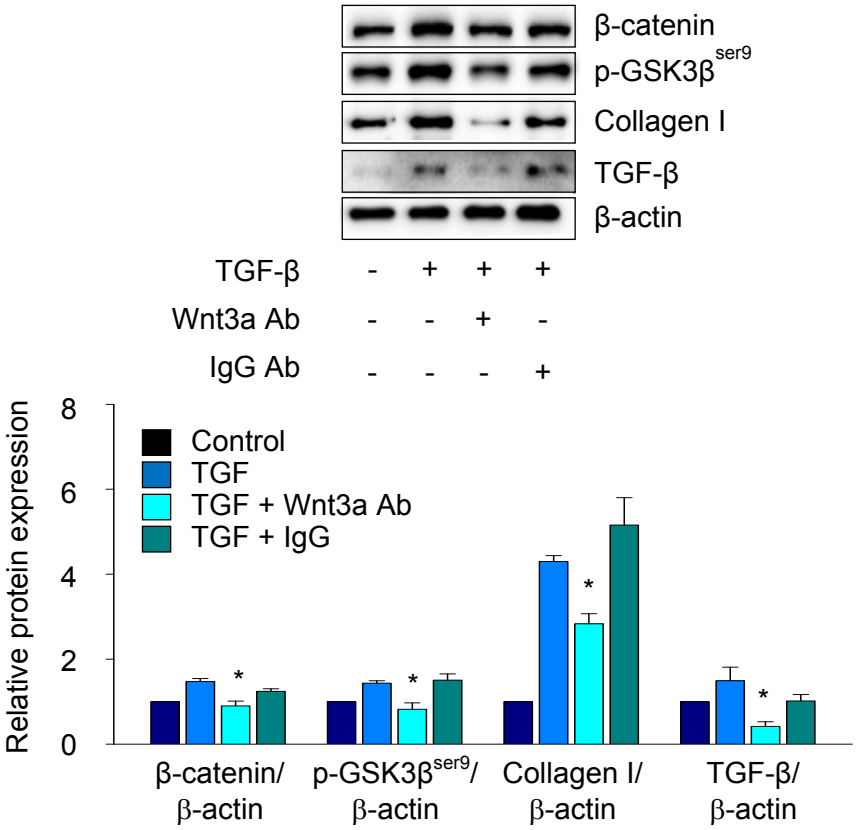

Figure 14. Effects of Wnt3a neutralization on CFs activation. The cells were treated with TGF-β (5 ng/ml) for 4 hours with or without Wnt3a-neutralizing antibodies (15μg/ml) and the expression levels of β-catenin, p-GSK3β^{ser9}, TGF-β, and collagen type I were examined by western blotting. Quantitative data were expressed as the means ± S.E.M. The similar results were obtained in at least 3 independent experiments. *p <0.05 compared to the TGF-β-treated control.

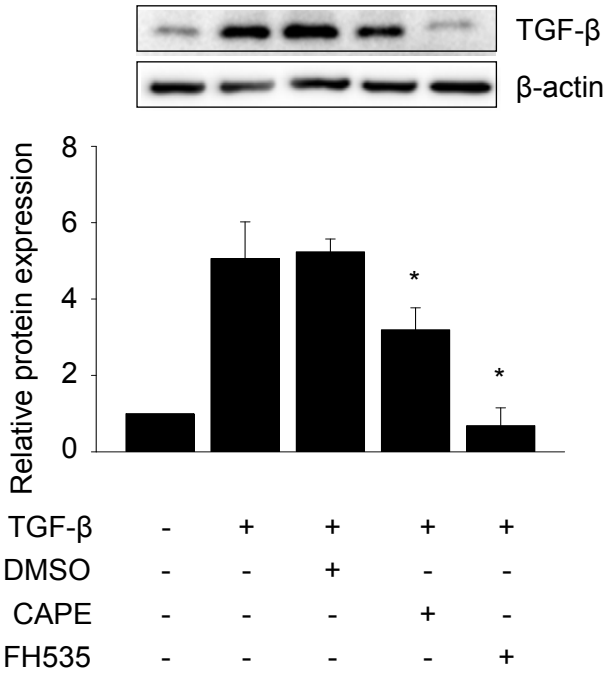

Figure 15. Inhibitory effects of NF-κB inhibitor and FH535 on TGF-β expression in TGF-β treated CFs. The cells were treated with TGF-β (5 ng/ml) for 4 hours in the presence of NF-κB inhibitor, CAPE (5μg/ml), an NF-kB inhibitor, and FH535 (15μM), a Wnt/β-catenin signaling inhibitor, and the expression levels of TGF-β were examined by western blotting. Quantitative data were expressed as the means ± S.E.M. The similar results were obtained in at least 3 independent experiments. **p* <0.05 compared to the TGF-β-treated control.

E. TGF-β/Wnt transactivation circuit in CF activation.

Data regarding the involvement Wnt signaling in the TGF-β-induced CF activation collectively indicated that the activation of TGF-β signaling increases the expression of one of the ligands of Wnt signaling, namely Wnt3a, and in return, the increased Wnt3a further increases the production of TGF-β, establishing a TGF-β/Wnt transactivation circuit as depicted in Figure 16.

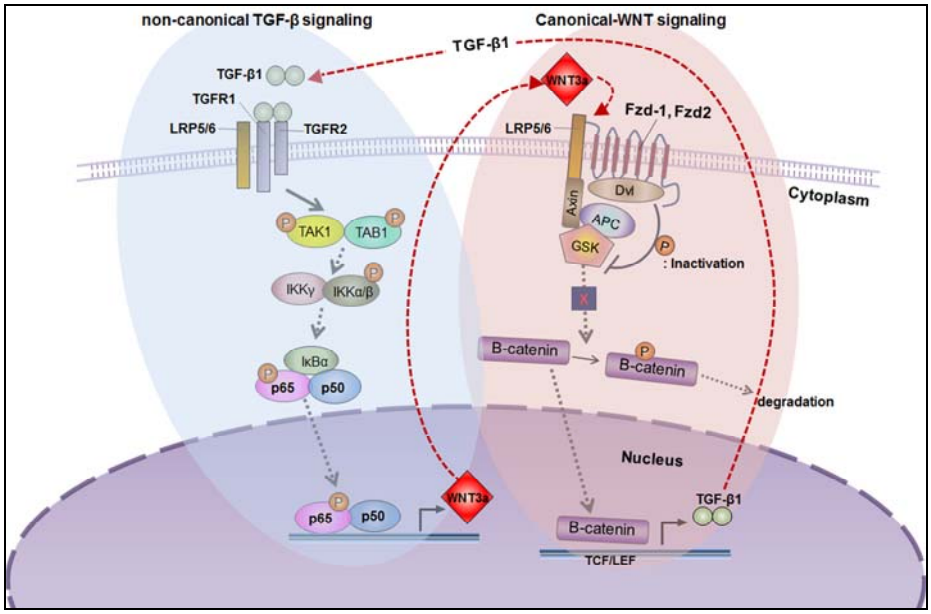

Figure 16. Schematic of the proposed TGF-β/Wnt transactivation circuit in TGF-β-induced CF activation. Schematic represents the transactivation circuits between the non-canonical Smad signaling pathway and the canonical Wnt signaling pathway.

6. Identification of a key miRNA that targets multiple receptors of the TGF-β/Wnt transactivation circuit

A. Screening of miRNAs targeting multiple receptors of the circuit

MicroRNAs are involved in virtually every aspect of numerous biological processes and a single miRNA can target multiple genes simultaneously. Thus, a key miRNA that affects both signaling pathways may exist and regulate the initiation and maintenance of the TGF-β/Wnt transactivation circuit. To find such miRNA(s), a miRNA-target mRNA prediction database (www.targetscan.org) was utilized. Because ligands of TGF-β and Wnt signaling can also be produced by cardiac cells other than CFs, downregulation of ligands in cardiac fibroblast may not be sufficient to disrupt the circuit *in vivo*. Thus, key receptors of the circuit were assumed as primary targets in the screening of miRNAs regulating the circuit. Fzd1 and Fzd2 have been implicated in cardiac fibrosis,[27] and their increased expression levels were also verified in the present study (Fig. 7). TGFβR1 is one of the main receptors for TGF-β signaling,[34] and LRP5 and LRP6 are well-known co-receptors for Wnt signaling.[35] Thus, these 5 receptors of the TGF-β and

Wnt signaling pathways were chosen as possible targets. Among the numerous miRNAs predicted to target each receptor (Tab. 1), only 2 miRNAs (miR-141-3p and miR-384-5p) were predicted to target 4 out of 5 receptors, namely, Fzd-1, Fzd-2, TGFβR1, and LRP6 (Fig. 17).

Table 1. MicroRNA families broadly conserved among vertebrates and predicted to target corresponding genes

WNT receptor (Frizzled, Fzd)		Fzd Co-receptor		TGFβreceptor
Fzd-1	**Fzd-2**	**LRP5**	**LRP6**	**TGFβR1**
miR-141	miR-141	x	miR-141	miR-141
miR-384	miR-384	x	miR-384	miR-384
miR-103-3p	miR-10-5p	miR-145-5p	miR-101-3p	let-7-5p
miR-122-5p	miR-129-5p	miR-23-3p	miR-10-5p	miR-101-3p
miR-125-5p	miR-140-3p	miR-375-3p	miR-124-3p	miR-105
miR-128-3p	miR-140-5p		miR-125-5p	miR-122-5p
miR-130-3p	miR-150-5p		miR-128-3p	miR-124-3p
miR-135-5p	miR-181-5p		miR-129-3p	miR-125-5p
miR-139-5p	miR-182		miR-132-3p	miR-128-3p
miR-1-3p	miR-490-3p		miR-135-5p	miR-130-3p
miR-145-5p	miR-96-5p		miR-138-5p	miR-132-3p
miR-146-5p			miR-148-3p	miR-133-3p
miR-148-3p			miR-155-5p	miR-135-5p
miR-150-5p			miR-15-5p	miR-139-5p
miR-15-5p			miR-181-5p	miR-140-3p
miR-17-5p			miR-183-5p	miR-140-5p
miR-183-5p			miR-18-5p	miR-142-3p
miR-184			miR-191-5p	miR-142-5p
miR-194-5p			miR-192-5p	miR-144-3p
miR-200bc-3p			miR-203-3p	miR-146-5p
miR-202-5p			miR-204-5p	miR-148-3p
miR-203-3p			miR-208-3p	miR-155-5p
miR-204-5p			miR-210-3p	miR-181-5p
miR-205			miR-21-5p	miR-182
miR-208-3p			miR-23-3p	miR-190-5p
miR-212-5p			miR-27-3p	miR-192-5p
miR-217-5p			miR-29-3p	miR-200bc-3p
miR-26-5p			miR-365-3p	miR-202-5p
miR-27-3p			miR-490-3p	miR-205
miR-29-3p			miR-499-5p	miR-208-3p
miR-34-5p			miR-7-5p	miR-216a-5p
miR-425-5p			miR-802-5p	miR-216b-5p
miR-455-3p			miR-96-5p	miR-221-3p
miR-499-5p				miR-22-3p
miR-9-5p				miR-24-3p
				miR-27-3p
				miR-29-3p
				miR-33-5p
				miR-338-3p
				miR-425-5p
				miR-489-3p
				miR-490-3p
				miR-499-5p
				miR-9-5p
				miR-96-5p

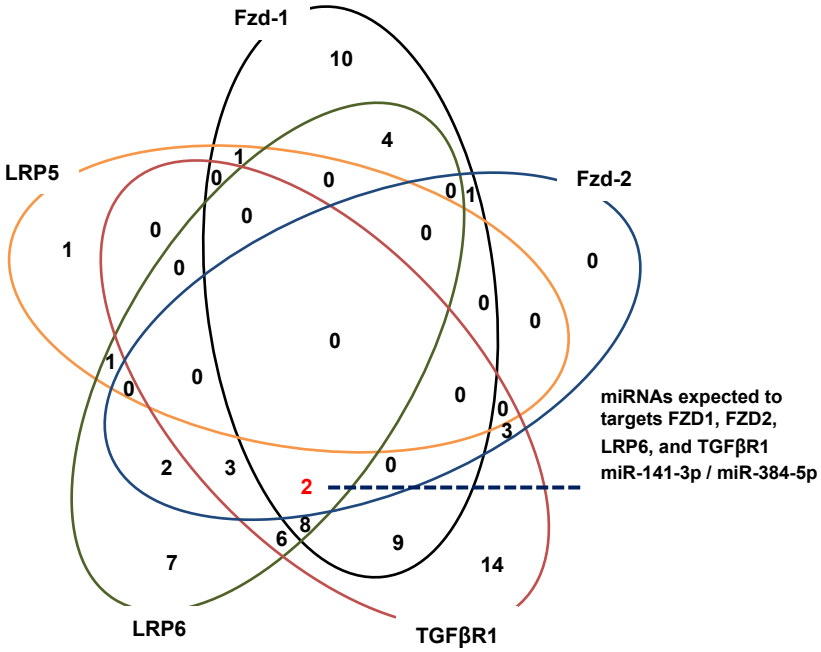

Figure 17. Selection of candidate miRNAs targeting multiple receptors of the circuit. MicroRNAs predicted to target the 5 key receptors of TGF-β and Wnt signaling pathway were analyzed to identify miRNAs targeting most of the receptors. The number in the Venn diagram indicates the number of miRNAs belonging to the corresponding intersection.

B. MicroRNA 384-5p targets Fzd-1, Fzd-2, TGFβR1, and LRP6

Subsequently, the effects of these miRNAs on the expression levels of the predicted target receptors were examined. As shown in Figure. 18, compared to miR-141-3p, miR-384-5p significantly suppressed the expression of the predicted targets. To further verify that the decreased expression of the 4 receptors was directly mediated by miR-384-5p, luciferase analysis was conducted (Fig. 19A). The luciferase activity significantly decreased in the presence of miR-384-5p in all cases, indicating that the 4 receptors were direct targets of miR-384-5p (Fig. 19B).

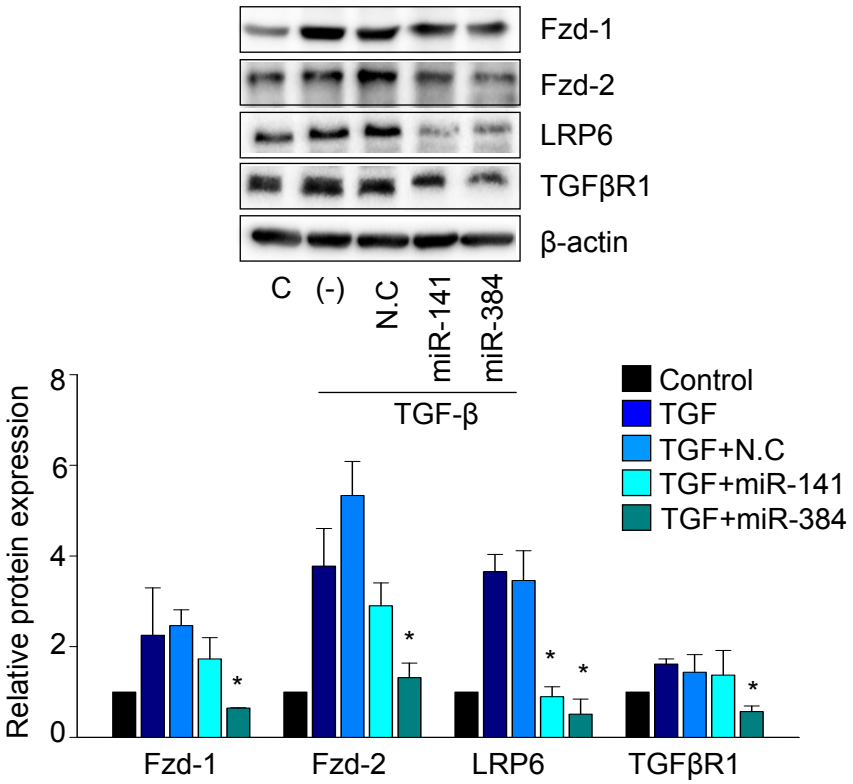

Figure 18. The effect of selected miRNAs on the expression of predicted target receptors. The cells were transfected with either 100 nM miR-141-3p or 100 nM miR-384-5p for 24 hr. The expression levels of predicted targets (Fzd1, Fzd2, TGFβR1, and LRP6) were examined by western blotting. *p<0.05 compared to the TGF-β-treated control. Quantitative data were expressed as the means ± S.E.M. The similar results were obtained in at least 3 independent experiments. **p* <0.05 compared to the TGF-β-treated control.

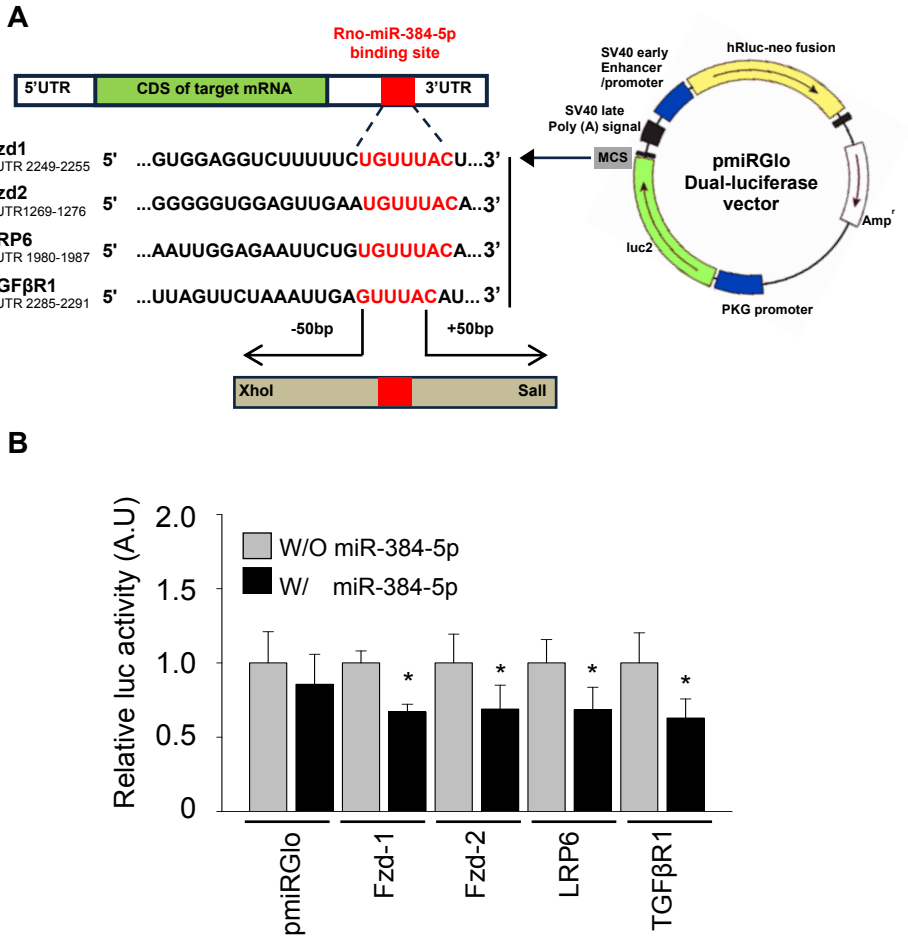

Figure 19. MicroRNA 384-5p directly targets the receptors of the circuit. (A) Schematic presentation of luciferase vector construction. The miR-384-5p-binding site in the 3'UTR of Fzd1, Fzd2, TGFβR1, and LRP6 was cloned into the pmirGLO vector using Xho I and Sal I restriction enzymes. (B) Luciferase vectors containing the miR-384-5p binding sites of each receptor were delivered to HeLa cells with or without co-delivery of miR-384-5p. Twenty-four hours after the transfection, luciferase activity was measured**.** Quantitative data were expressed as the means ± S.E.M. The similar results were obtained in at least 3 independent experiments. **p* <0.05 compared to the matching pair.

C. Effect of fibrogenic stimuli on miR-384-5p expression

To verify the possibility that miR-384-5p expression was altered during I/R-injury and thereby affected the expression of these receptors and the formation of the TGF-β/Wnt transactivation circuit, the expression levels of miR-384-5p was examined in the I/R-injured heart and in TGF-β-treated primary CFs. As shown in Figure 20A, the expression of miR-384-5p significantly decreased at 3 and 7 days after the injury, and 24 hours of the TGF-β treatment also significantly decreased the expression levels of miR-384-5p in the primary CFs (Fig. 20B). These data strongly suggest that miR-384-5p is a key regulator of the TGF-β/Wnt transactivation circuit and that downregulation of miR-384-5p during I/R-injury promotes CF activation and subsequent cardiac fibrosis by enhancing the expression of key receptors involved in the circuit.

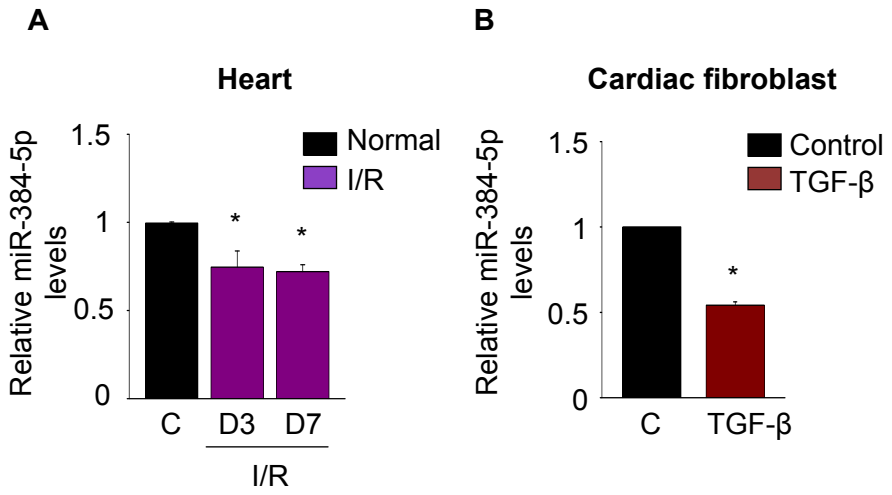

Figure 20. The expression of miR-384-5p in I/R-injured heart and TGF-β-treated CFs. The expression levels of miR-384-5p in the I/R-injured heart and TGF-β-treated CFs were examined. (A) Three and seven days after the injury, the heart tissue was collected, and the expression of miR-384-5p was detected by real-time PCR. Normal heart tissue was used as a control. (B) Primary CFs were treated with 5 ng/ml TGF-β for 24 hours, and the expression of miR-384-5p was detected by real-time PCR. Quantitative data were expressed as the means ± S.E.M. The similar results were obtained in at least 3 independent experiments. *$p<0.05$ compared to the control

7. Effect of miR-384-5p on TGF-β and Wnt signaling

A. MicroRNA 384-5p inhibits TGF-β signaling pathway.

The effects of miR-384-5p on the TGF-β and Wnt signaling pathway were examined. As shown in Figure 21, miR-384-5p inhibited activation of both the Smad pathway (Fig. 21A) and non-Smad pathway (Fig. 21B) as evidenced by the decreased expression of p-Smad and p-P65, respectively.

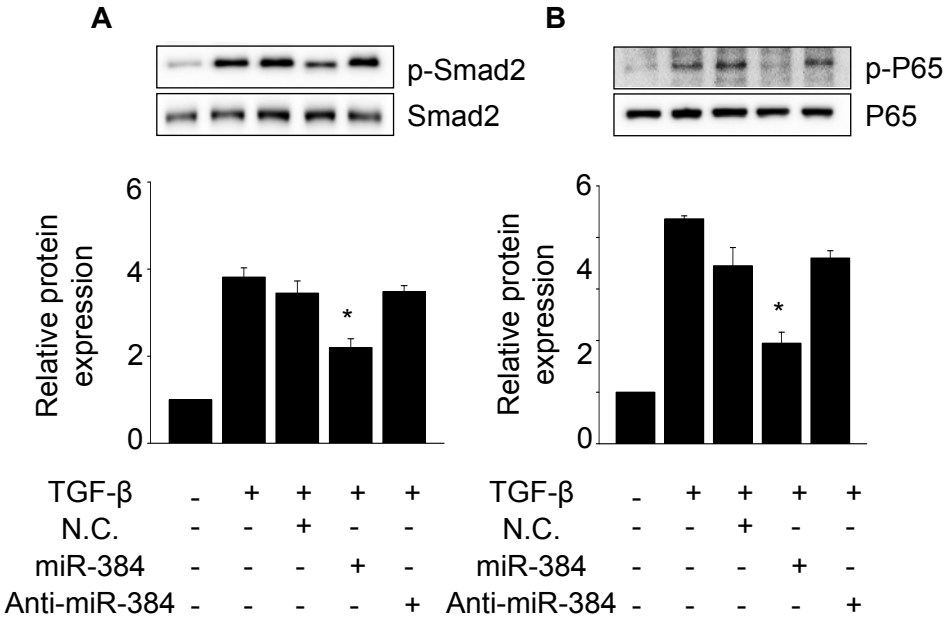

Figure 21. The effect of miR-384-5p on TGF-β signaling pathway. The cells were transfected with 100 nM miR-384-5p or anti-miR-384-5p for 24 hours and then treated with TGF-β for an additional 24 hours. The expression levels of signaling molecules in the (A) Smad pathway and (B) non-Smad pathway were examined. Quantitative data were expressed as the means ± S.E.M. The similar results were obtained in at least 3 independent experiments. **p* <0.05 compared to the TGF-β-treated control.

B. MicroRNA 384-5p inhibit canonical Wnt signaling pathway

Regarding of miR-384-5p on the Wnt and β-catenin pathway, miR-384-5p decreased phosphorylation of GSK3β^{ser9} and β-catenin (Fig. 22). This observation indicated that miR-384-5p suppressed TGF-β-induced activation of Wnt/β-catenin signaling in the primary CFs. Moreover, the immunocytochemical data showed that miR-385-5p prominently attenuated TGF-β-induced nuclear translocation of β-catenin (Fig. 23).

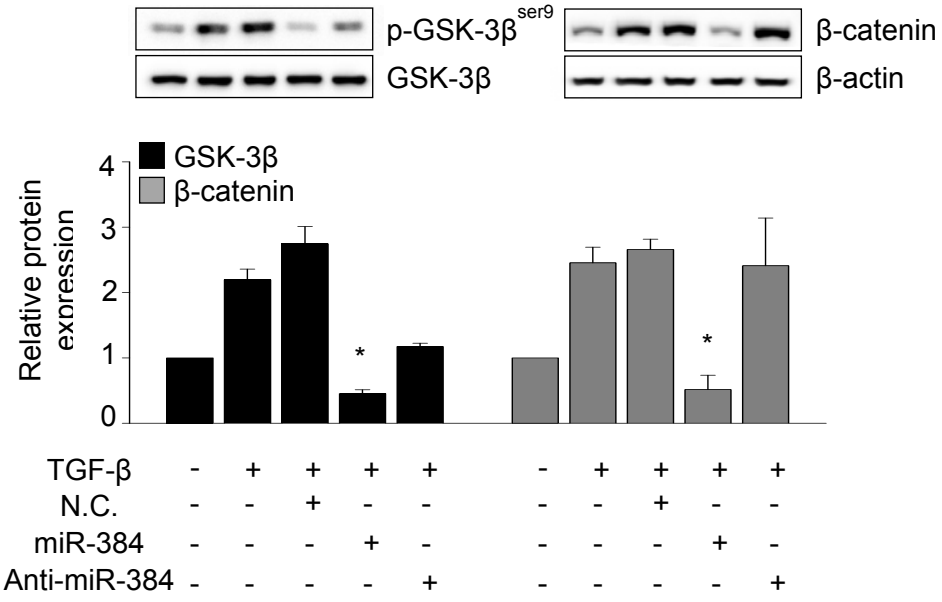

Figure 22. The effects of miR-384-5p on canonical Wnt signaling pathway. The cells were transfected with 100 nM miR-384-5p or anti-miR-384-5p for 24 hours and then treated with TGF-β for an additional 24 hours. The expression levels of signaling molecules in the Wnt/β-catenin pathway were examined. N.C.: negative control scrambled miRNA. Quantitative data were expressed as the means ± S.E.M. The similar results were obtained in at least 3 independent experiments. **p* <0.05 compared to the TGF-β-treated control.

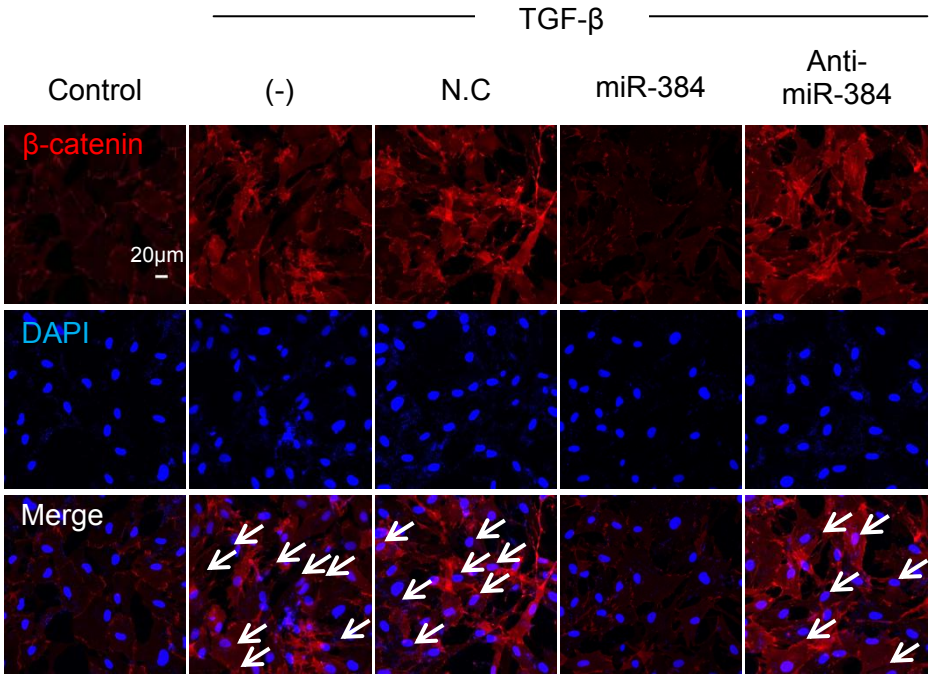

Figure 23. The inhibitory effect of miR-384-5p on nuclear translocation of β-catenin. The cells were transfected with either 100 nM miR-384-5p or 50 nM anti-miR-384-5p for 24 hours and then exposed to 5 ng/ml TGF-β for an additional 24 hours. The expression of β-catenin was visualized by immunocytochemistry. Nuclei were stained with DAPI. N.C.: negative control scrambled miRNA. White arrows indicate nuclear localized β-catenin. Scale bar represents 20 μm.

8. Effect of miR-384-5p on the TGF-β-induced activation of CFs

A. MicroRNA 384-5p inhibits the expression of CFs activation marker

To examine whether miR-384-5p indeed suppressed TGF-β-induced activation of primary CFs, the cells were transfected with 100 nM miR-384-5p for 24 hours and then exposed to 5 ng/ml TGF-β for an additional 24 hours. The delivery of exogenous miR-384-5p significantly decreased the expression of both α-SMA and collagen type I (Fig. 24). Immunocytochemical staining of α-SMA also indicated that miR-384-5p clearly suppressed the expression of α-SMA (Fig. 25). These data suggested that TGF-β-induced CF activation was significantly attenuated by miR-384-5p.

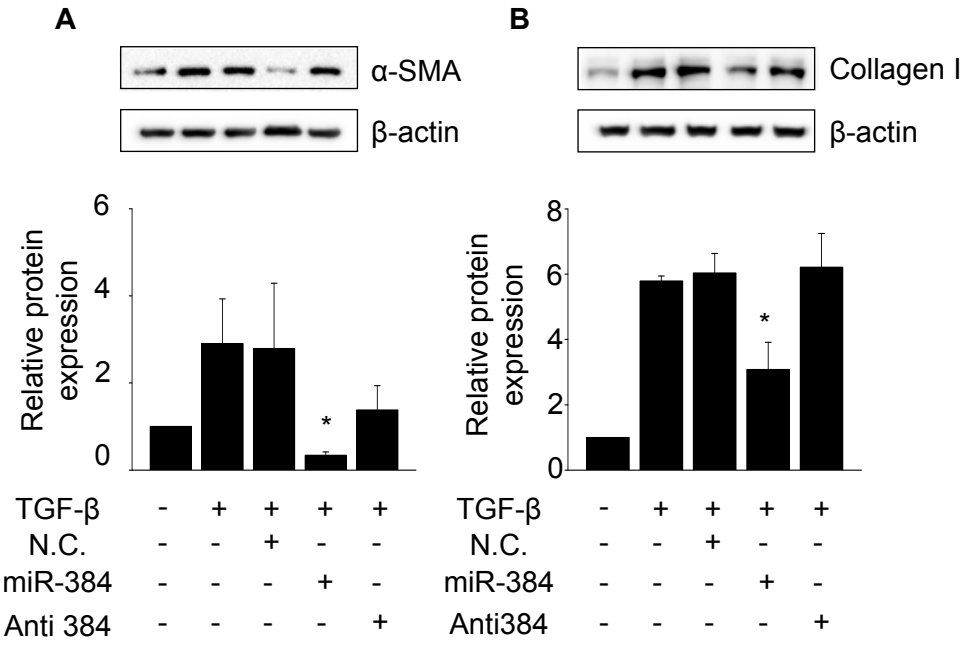

Figure 24. The miR-384-5p suppresses α-SMA and collagen type I expression. The cells were transfected with 100 nM miR-384-5p for 24 hours. The expression of (A) α-SMA and (B) collagen type I (Collagen I) was examined by western blotting. N.C.: negative control scrambled miRNA; Anti 384: anti-miR-384-5p. Quantitative data were expressed as the means ± S.E.M. The similar results were obtained in at least 3 independent experiments. **p* <0.05 compared to TGF-β-treated control.

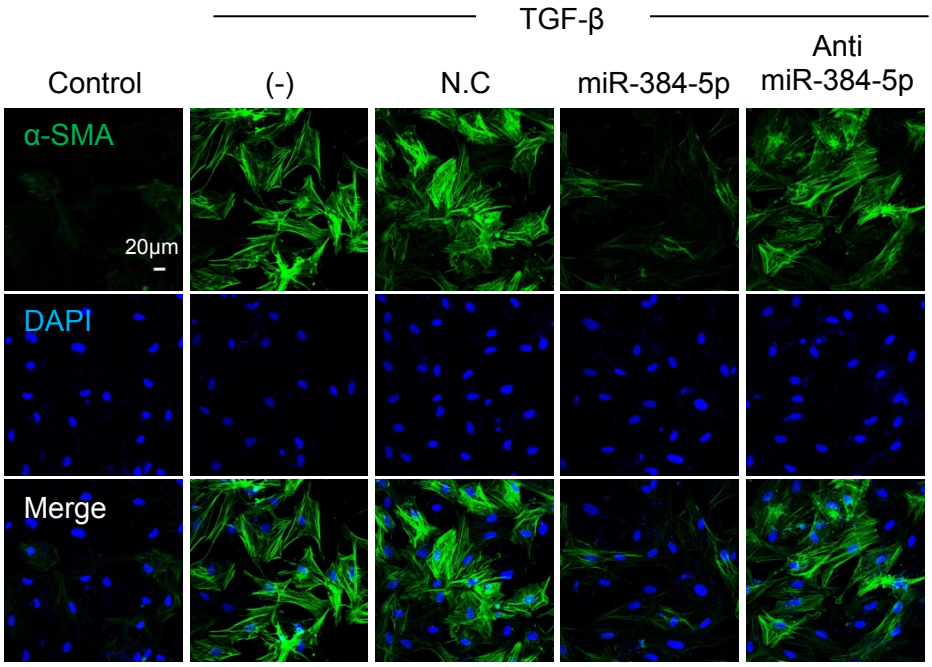

Figure 25. Immunocytochemical staining of α-SMA. The cells were transfected with 100 nM either miR-384-5p or anti-miR-384-5p for 24 hours and exposed to 5 ng/ml TGF-β for an additional 24 hr. The expression of α-SMA was visualized by immunocytochemistry. N.C.: negative control scrambled miRNA. Nuclei were stained with DAPI. Scale bar represents 20 μm.

B. MicroRNA 384-5p suppresses proliferation, migration and contractility of TGF-β-stimulated CFs

In response to chemokines released at the site of injury, activated CFs or myoFBs migrate to the damaged area, restoring cellularity.[1] The results of the migration assays indicated that miR-384-5p suppressed migration of the TGF-β-treated CFs (Fig. 26). In addition, miR-384-5p significantly inhibited CFs proliferation as well (Fig. 27). Lastly, collagen gel contraction analysis was performed to examine the effect of miR-384-4p on collagen contractility. The data indicated that miR-384-5p significantly attenuated the TGF-β-induced collagen contractility of the primary CFs (Fig. 28).

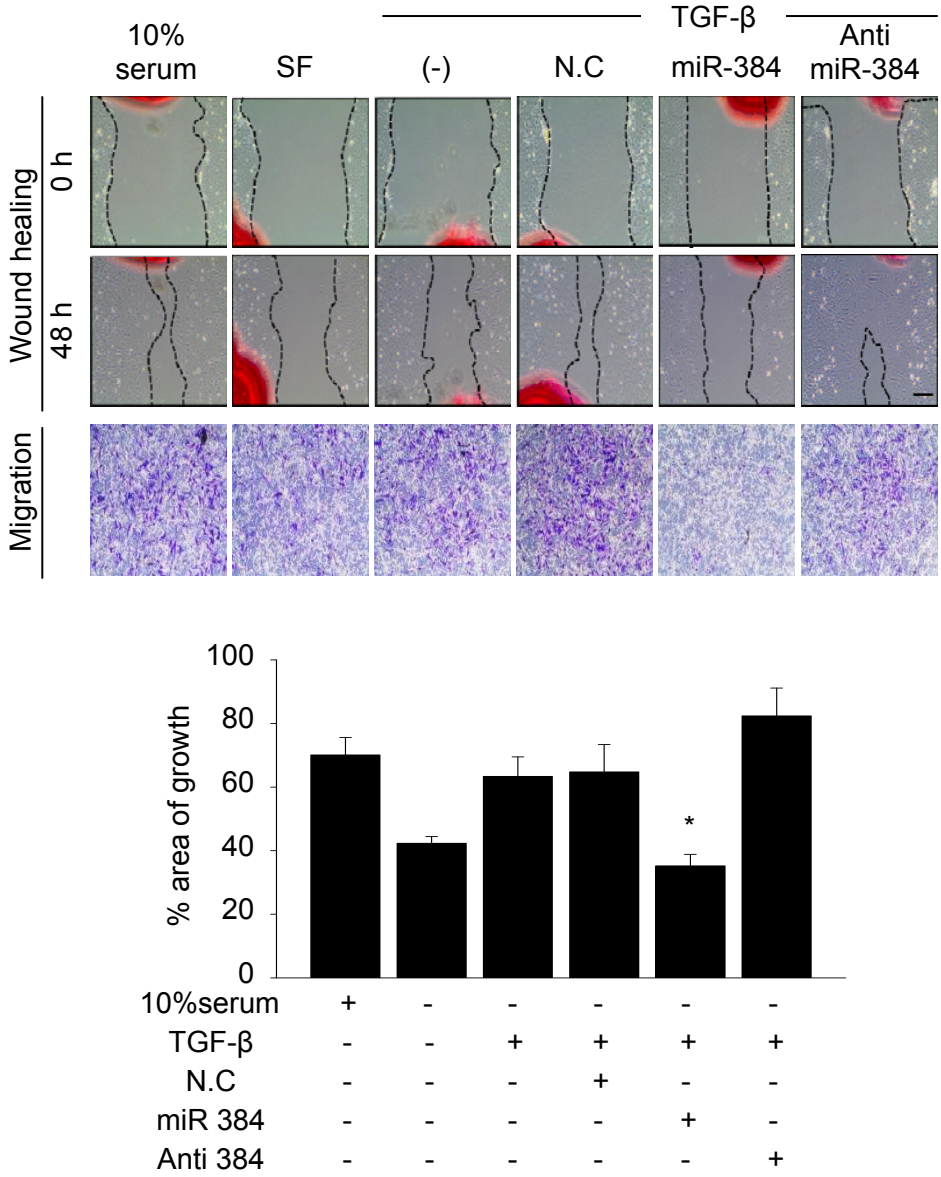

Figure 26. Effect of miR-384-5p on TGF-β-induced migration of CFs. For the wound-healing analysis, the cells were transfected with 100 nM miR-384-5p for 24 hours. The wound was created by scratching the surface of the culture dish with a yellow pipette tip. The images of the wounds were

obtained at 0 and 48 hours. The area between the wound edges was measured and compared among the groups. Quantitative data were expressed as the means ± S.E.M. The similar results were obtained in at least 3 independent experiments. *p <0.05 compared to TGF-β-treated control. For the migration analysis, the cells were seeded in the upper chambers of Transwells and transfected with either 100 nM miR-384-5p or 100 nM anti-miR-384-5p for 24 hr. The cells were further treated with TGF-β for an additional 24 hours. Migrated cells were stained with crystal violet. N.C.: negative control scrambled miRNA; Anti 384: anti-miR-384-5p. Scale bar represents 2 mm.

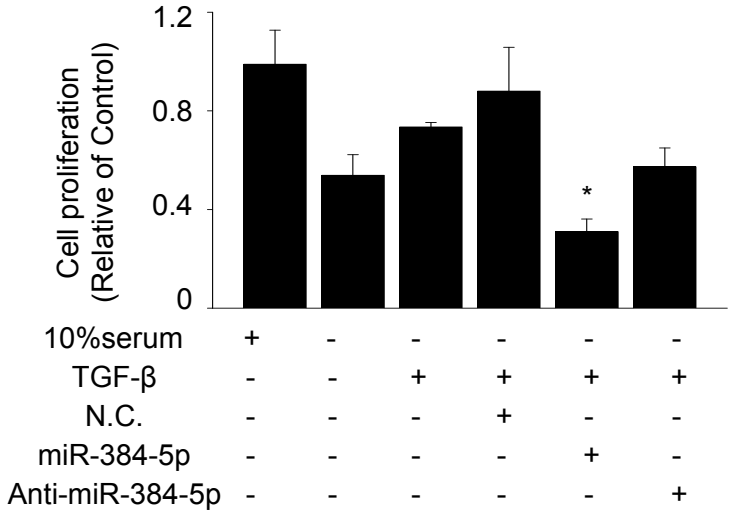

Figure 27. Effect of miR-384-5p on CF proliferation. CFs were transfected with miR-384-5p or anti-miR-384-5p at concentrations of 100nM and 50nM, respectively, for 24 hours. After transfection, cell were starved for 12 hours and then treated with TGF-β for 48 hours. Cell proliferation was measured using a CCK-8 assay kit. N.C.: negative control scrambled miRNA. Quantitative data were expressed as the means ± S.E.M. The similar results were obtained in at least 3 independent experiments. **p* <0.05 compared to TGF-β treated group.

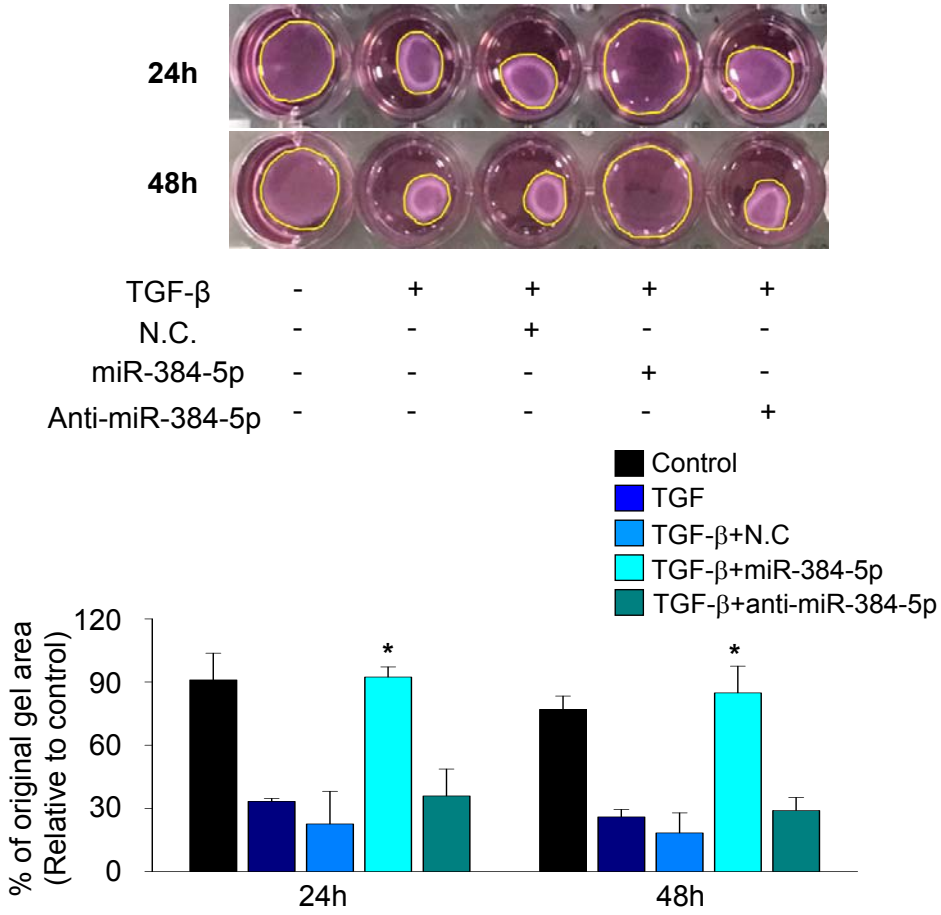

Figure 28. Effect of miR-384-5p on collagen gel contractility. Cardiac fibroblast-containing collagen gels were serum-starved for 12 hours. After starvation, gels were stimulated with TGF-β (5 ng/ml) for 48 hours and photographed at 24 hour and 48 hour. The size of the gels were measured and analyzed. N.C.: negative control scrambled miRNA. Quantitative data were expressed as the means ± S.E.M. The similar results were obtained in at least 3 independent experiments. **p* <0.05 compared to the TGF-β treated group.

9. Effect of miR-384-5p on cardiac fibrosis following I/R-injury

A. MicroRNA 384-5p inhibits I/R-injury-induced cardiac fibrosis

To investigate the therapeutic effect of miR-384-5p *in vivo*, exogenous miR-384-5p (10 μg/head) was delivered to the heart following I/R-injury. Up to 7days after the injury, the expression of miR-384-5p was well maintained compared to the I/R-injured heart without exogenous miR-384-5p delivery (Fig. 29). The expression levels of Fzd-1, Fzd-2, LRP6, and TGFβR1 significantly decreased with miR-384-5p delivery to the I/R-injured heart (Fig. 30). Most importantly, delivery of exogenous miR-384-5p significantly attenuated progression of cardiac fibrosis as evidenced by the significantly decreased size of the fibrotic area (Fig. 31A) and well-maintained left ventricular (LV) wall thickness (Fig. 31B). These data indicated that exogenous miR-384-5p that was delivered to heart following I/R-injury significantly suppressed cardiac fibrosis.

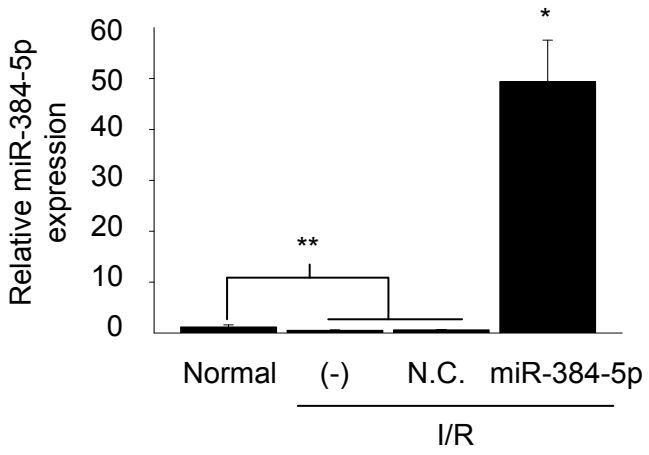

Figure 29. The expression levels of miR-384-5p in I/R-injured heart. The *in vivo* expression levels of miR-384-5p were detected by real time PCR at 14 days after the injury. MicroRNA 384-5p (10 μg/head) was injected to the heart right after I/R injury. N.C.: negative control scrambled miRNA. Quantitative data were expressed as the means ± S.D. of data collected from 5 animals. ***p* <0.05 compared to untreated control. **p* <0.05 compared to I/R control.

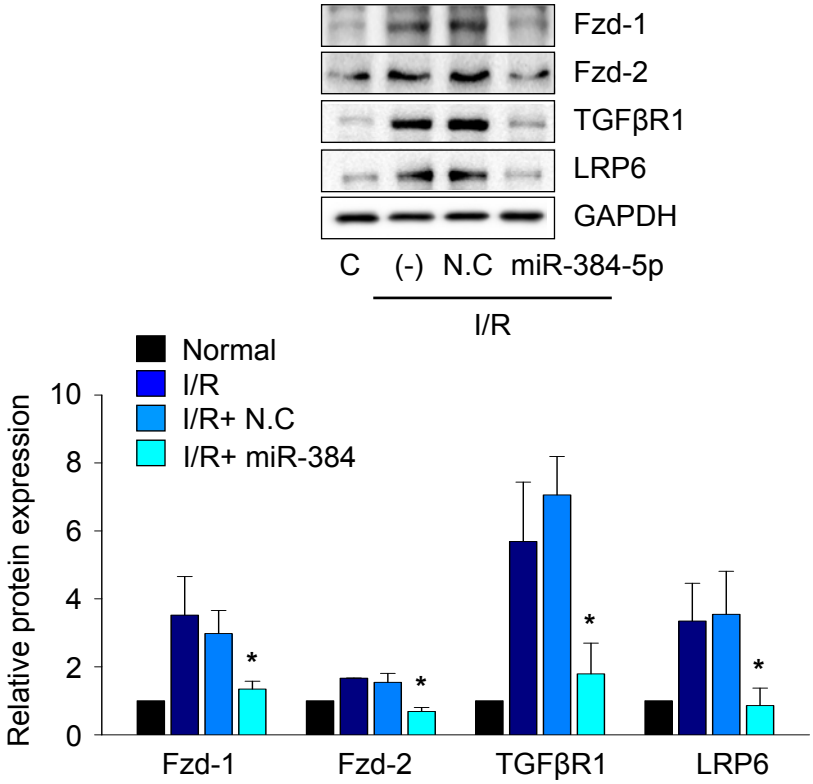

Figure 30. The effect of exogenous miR-384-5p on the expression of the key receptors following I/R-injury. The effect of exogenous miR-384-5p on the expression of the key receptors (Fzd-1, Fzd-2, LRP6, and TGFβR1) following I/R-injury (7 days after the injury) was detected by western blotting. N.C.: negative control scrambled miRNA. Quantitative data were expressed as the means ± S.E.M. The similar results were obtained in at least 3 independent experiments. **p* <0.05 compared to the TGF-β treated CFs.

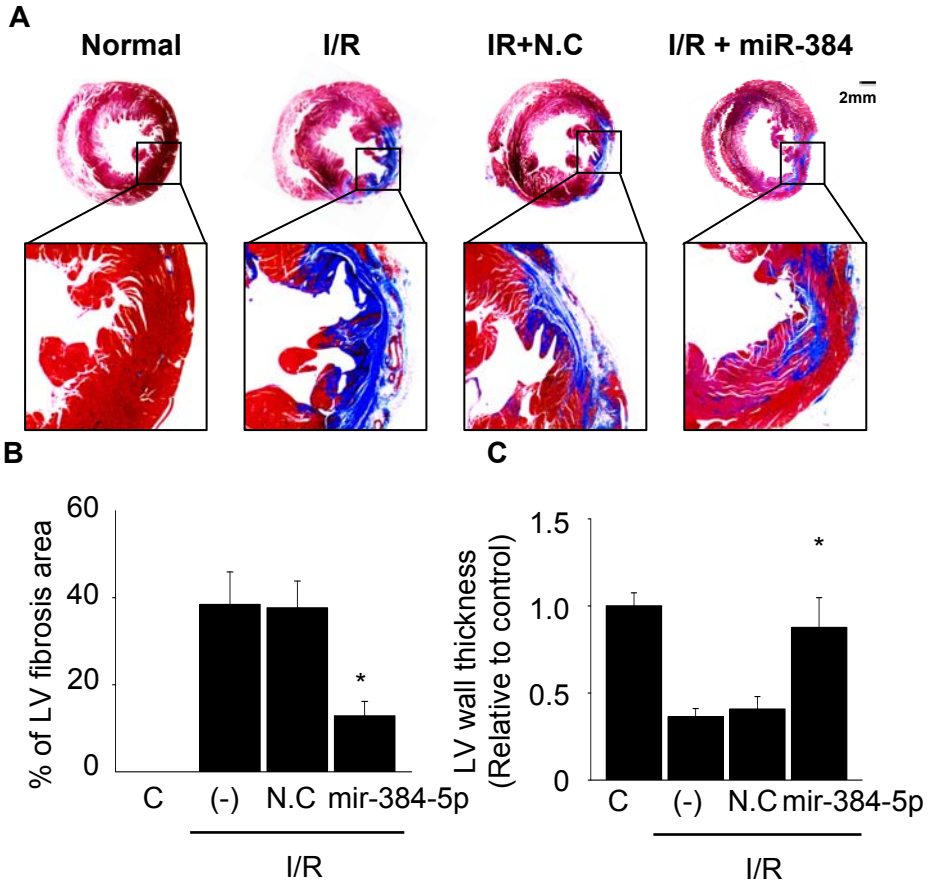

Figure 31. MicroRNA 384-5p attenuates cardiac fibrosis following I/R-injury. (A) Representative images of Masson's trichrome-stained sections demonstrating fibrosis. (B) The area of fibrosis and (C) left ventricular (LV) wall thickness were also measured. N.C.: negative control scrambled miRNA. Quantitative data were expressed as the means ± S.E.M. of the data collected from 5 animals. **p* <0.05 compared to I/R.

10. Screening of small molecules that increase endogenous miR-384-5p expression.

A. Drug 145 augments the expression of endogenous miR-384-5p

Although the anti-fibrotic effect of exogenous miR-384-5p has been demonstrated, therapeutic application of exogenous miRNAs has several limitations such as low cellular uptake, off-target effects, and instability in serum.[36] Therefore, as an alternative to direct *in vivo* application of exogenous miRNAs, I attempted small molecule-mediated regulation of endogenous miRNAs in the present study. Using an in-house small-molecule library that mainly comprised commercially available inhibitors of six kinase subfamilies,[37] a small molecule that upregulates endogenous miR-384-5p expression was identified. Among the small molecules tested, small molecule number 145 (Drug 145; D145) most significantly increased the exogenous expression of miR-384-5p in CFs (Fig. 32), and the identity of small molecule 145 was azathioprine, a well-known immunosuppressive agent.[38] To visualize D145-induced endogenous miR-384-5p expression, molecular beacons that consisted of Cy3-modified long, complementary nucleotides to miR-384-5p and black hole quencher (BHQ1)-modified short, partial miR-384-5p nucleotides were used (Fig. 33). When the CFs with the molecular beacon

were treated with 10μM D145 for 24hours, the Cy3 signal in the primary CFs prominently increased (Fig. 34), indicating that D145 increased the level of endogenous miR-384-5p in the primary CFs. When the cells were treated with increasing concentrations of D145 (10, 15, and 20 μM), the expression of endogenous miR-384-5p was significantly increased at concentrations of 10 μM or higher. However, no significant concentration-dependent effect was observed (Fig. 35).

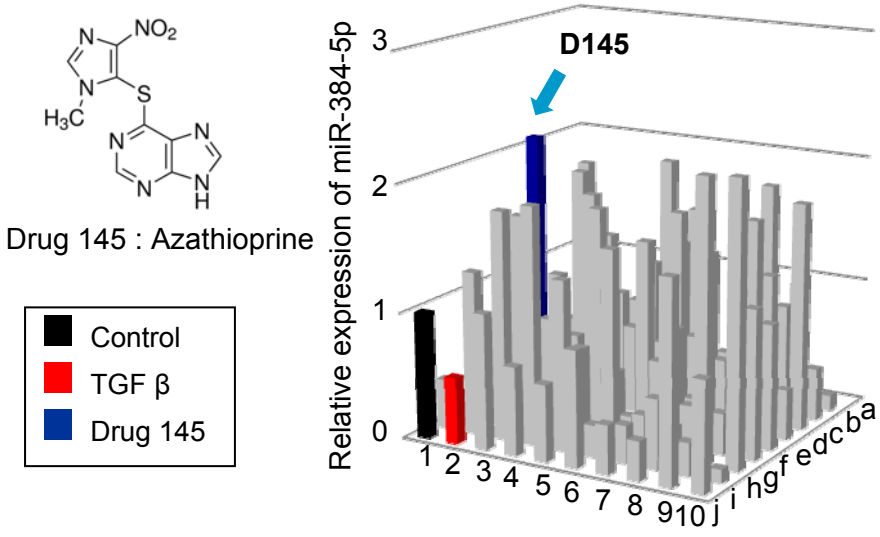

Figure 32. Screening of small molecules for induction of endogenous miR-384-5p expression. CFs were treated with an in-house small-molecule library that mainly consisted of commercially available inhibitors of six kinase subfamilies (10 μM each) for 48 hours. The expression level of miR-384-5p was determined by real-time PCR.

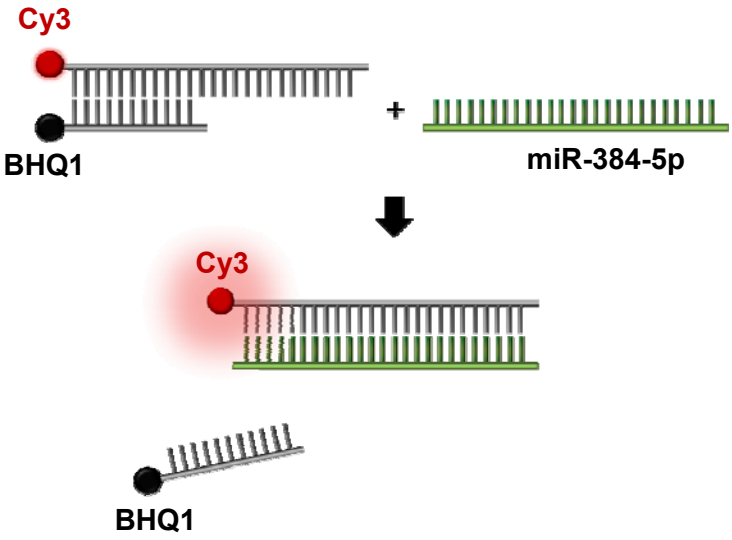

Figure 33. Schematic showing the miRNA detection mechanism of molecular beacon. The schematics shows the working mechanism of the molecular beacon for detecting miR-384-5p expression. When miR-384-5p is present, the binding between Cy3-modified strand and BHQ1-modified strand is hindered. Consequently, fluorescent resonance energy transfer (FRET) is lost, and Cy3 emits fluorescence. BHQ1: black hole quencher 1.

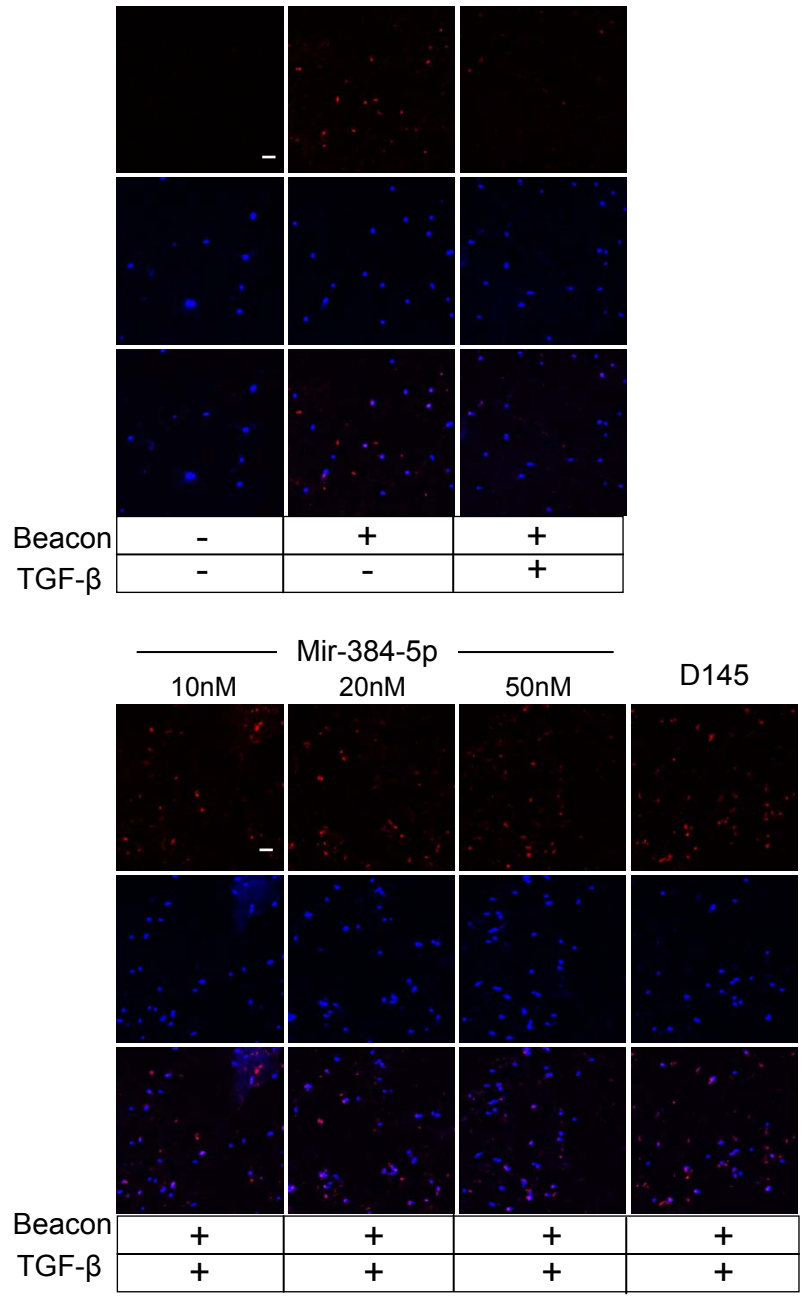

Figure 34. D145-induced increase of miR-384-5p detected by molecular beacon. (A) To visualize the effect of TGF-β on the expression level of endogenous miR-384-5p, the cells were treated with or without TGF-β for 48

hours. The Cy3-fluorescence, which indicates the presence of endogenous miR-384-5p, was detected. (B) The cells were treated with either increasing concentrations of miR-384-5p or 10 μM D145 as indicated for 48 hours, and the Cy3-fluorescence from miR-384-5p bound molecular beacon was detected by using a confocal microscope Scale bar represents 20 μm.

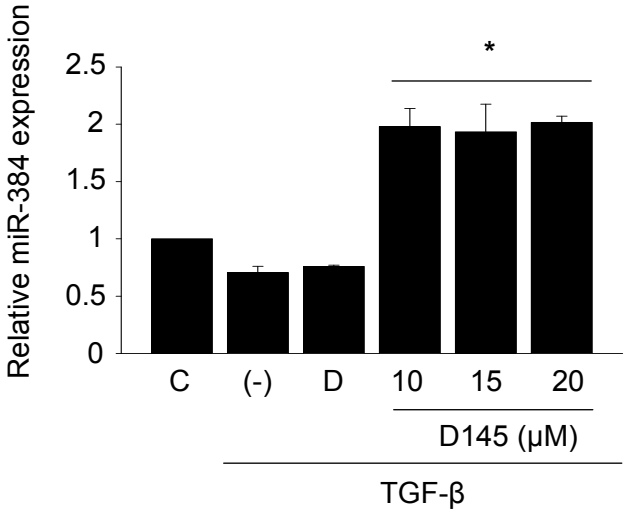

Figure 35. Effect of D145 on miR-384-5p expression in CFs. The cells were treated with increasing concentrations of D145 in the presence of TGF-β (5 ng/ml) as indicated for 48 hours. The expression of miR-384-5p was determined by real-time PCR. Quantitative data were expressed as the means ± S.E.M. The similar results were obtained in at least 3 independent experiments. D: DMSO used as vehicle. **p* <0.05 compared to TGF-β-treated CFs.

11. Underlying mechanism of D145-induced increase in endogenous miR-384-5p

A. The effect of D145 on endogenous miR-384-5p may not be due to increased transcription activity of the miR-384-5p promoter

To investigate the underlying mechanism of the D145-induced increase in miR-384-5p, a promoter analysis using a 3000-bp fragment of the rno-miR-384-5p promoter was conducted (Fig. 36). According to the luciferase activity result, no significant effect of the D145 treatment on the luciferase activity was observed. This result indicates that the observed increase in miR-384-5p by D145 may be due to miRNA stability regulation,[39] or increased processing of primary miRNA (pri-miRNA)[40] rather than increased transcriptional activity of the miR-384-5p promoter. To further determine whether the effect of D145 was miR-384-5p-specific, the expression levels of randomly chosen miRNAs were examined. D145 had no significant effect on the expression levels of miRNAs other than miR-384-5p (Fig. 37), suggesting that the effect of D145 was specific to miR-384-5p.

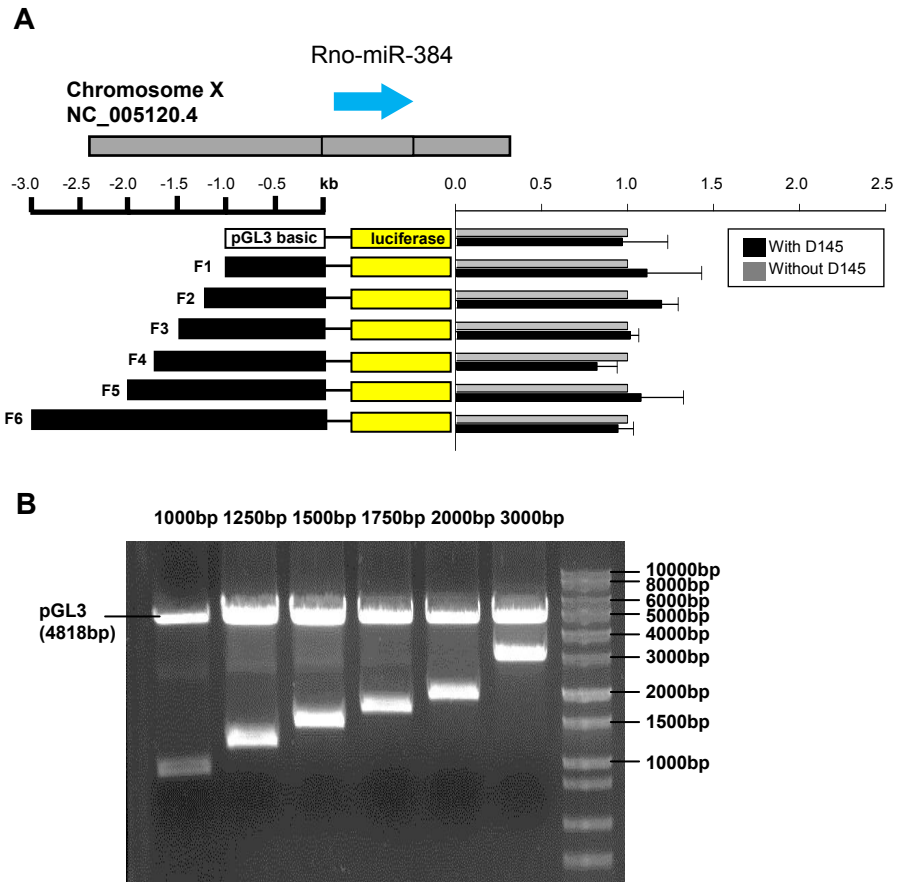

Figure 36. Promoter assay using 3000 bp-long fragment of rno-miR-384-5p promoter. (A) For the promoter analysis, a 3000-bp sequence upstream of the start codon of rno-miR-384 was used. (B) The size confirmation after enzymatic digestion is shown on the bottom panel.

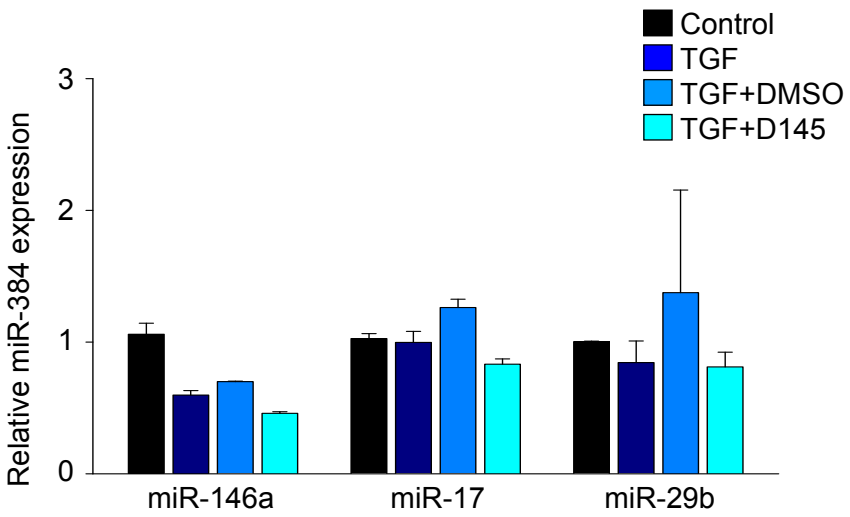

Figure 37. Effect of D145 on randomly chosen miRNAs other than miR-384-5p The cells were serum starved for 12 hours. After starvation, 10μM D145 were treated for 1 hour. After 1 hour, 5ng/ml TGF-β were added and incubated for 24 hours. Expression levels of randomly chosen miRNAs were evaluated by quantitative real time PCR. Quantitative data were expressed as the means ± S.E.M. The similar results were obtained in at least 3 independent experiments.

12. Effect of D145 on the TGF-β/Wnt transactivation circuit

A. D145 downregulates the expression of the receptors of the circuit.

To examine whether the D145-induced increase in endogenous miR-384-5p could be translated into actual downregulation of the receptors of interest, the cells were treated with 10 μM D145 with or without anti-miR-384-5p and the expression levels of Fzd-1, Fzd-2, TGFβR1, and LRP6 was detected by western blot. According to the data, D145 significantly decreased the expression of those receptors altogether (Fig. 38). Importantly, the effect of D145 was abrogated by anti-miR-384-5p treatment, demonstrating that the effect of D145 was mediated by the enhanced expression of endogenous miR-384-5p.

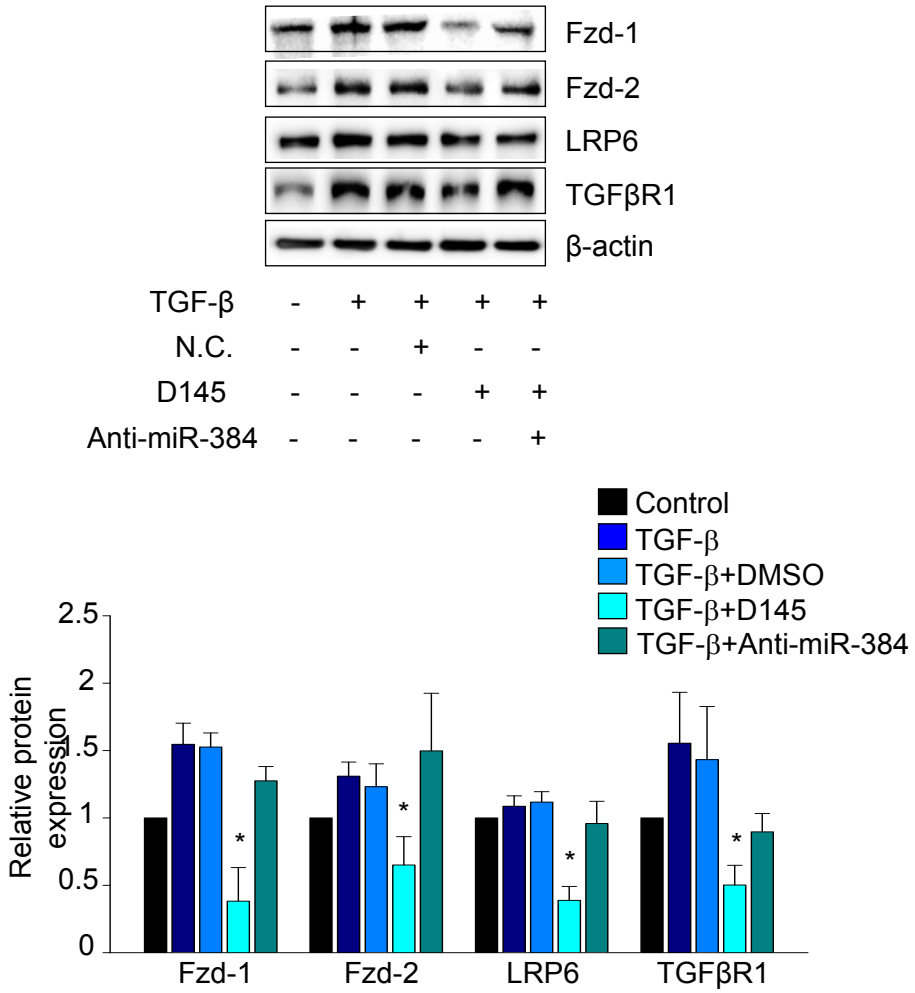

Figure 38. Effects of D145 on the expression of multiple receptors. The cells were treated with 10 μM of D145 for 24 hours with or without anti-miR-384-5p pretreatment. The expression of key receptors (Fzd1, Fzd2, TGFβR1, and LRP6) was examined by western blot. N.C.: negative control scrambled miRNA. Quantitative data were expressed as the means ± S.E.M. The similar results were obtained in at least 3 independent experiments. **p* <0.05 compared to the TGF-β treated CFs.

B. D145 inhibits both TGF-β and Wnt signaling pathway

The effect of D145 on the TGF-β and Wnt signaling pathways was examined. D145 inhibited activation of both the Smad pathway and non-Smad pathway as evidenced by the decreased expression of p-Smad and p-P65, indicating decreased NF-kB activity (Fig. 39). Regarding the Wnt/β-catenin pathway, D145 decreased phosphorylation of GSK3β^{ser9} and β-catenin (Fig. 40). Additionally, immunocytochemical staining demonstrated that D145 prominently attenuated TGF-β-induced nuclear translocation of β-catenin (Fig. 41). These results indicated that the effect of D145 was quite similar to that of exogenous miR-384-5p.

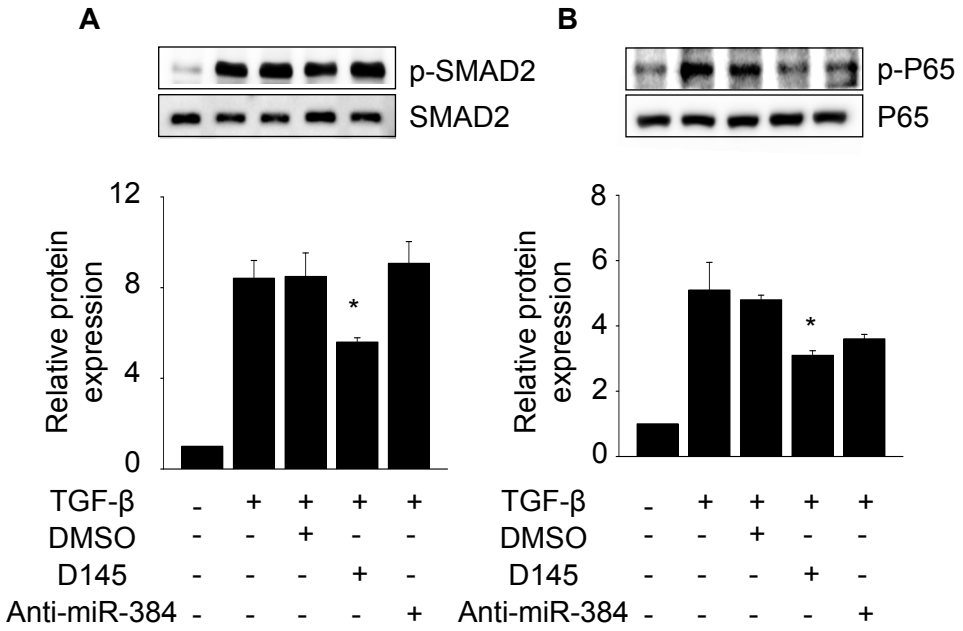

Figure 39. D145 suppresses TGF-β signaling pathway. The cells were transfected with 50 nM anti-miR-384-5p for 24 hr. After 24hr, the medium was changed to fresh 10% FBS DMEM. After 20 hours, the cells were starved for 12 hours and, cells were treated 10μM D145 for 1 hour. After that, 5ng/ml TGF-β were added and incubated for 30min. The expression levels of signaling molecules in the (A) Smad pathway and (B) non-Smad (P65-mediated pathway) pathway were examined. Quantitative data were expressed as the means ± S.E.M. The similar results were obtained in at least 3 independent experiments. **p* <0.05 compared to the TGF-β treated CFs.

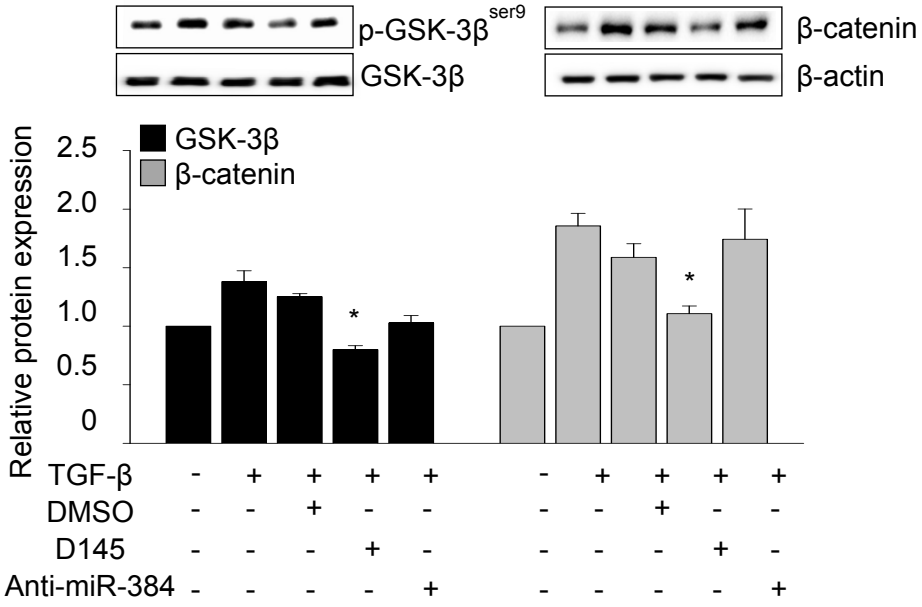

Figure 40. D145 suppresses canonical Wnt signaling pathway. The cells were transfected with 50 nM anti-miR-384-5p for 24 hr. After 24hr, the medium was changed to fresh 10% FBS DMEM. After 20 hours, the cells were starved for 12 hours and, cells were treated 10μM D145 for 1 hour. After that, 5ng/ml TGF-β were added and incubated for 30min. The expression levels of signaling molecules of the Wnt/β-catenin pathway were examined. Quantitative data were expressed as the means ± S.E.M. The similar results were obtained in at least 3 independent experiments. **p* <0.05 compared to the TGF-β treated CFs.

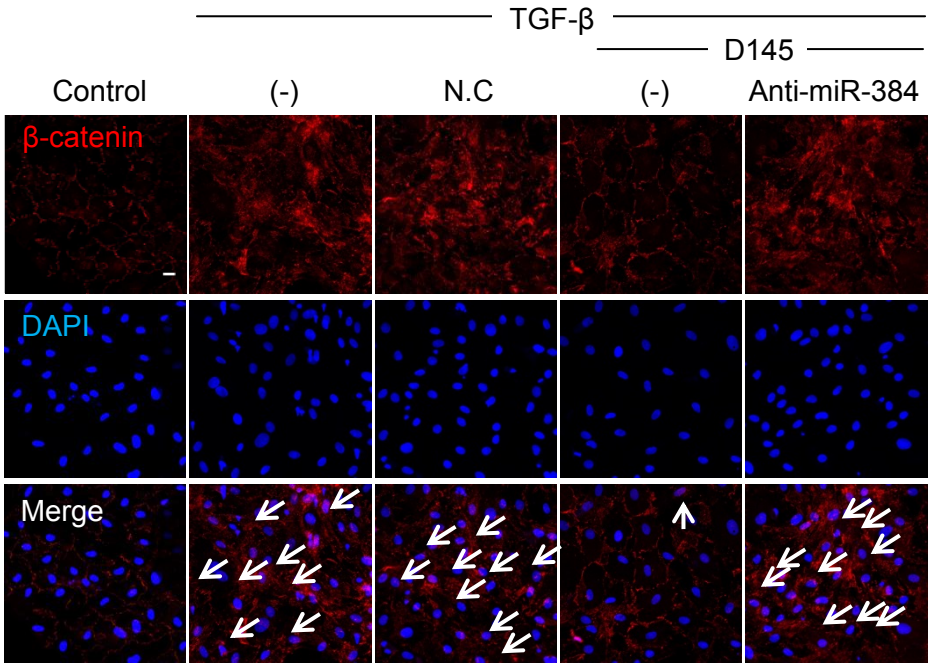

Figure 41. D145 inhibits TGF-β-induced nuclear translocation of β-catenin. The cells were treated with 10 μM D145 for 24 hours with or without the anti-miR-384-5p pretreatment. The expression levels of β-catenin was visualized by immunocytochemistry. Nuclei were stained with DAPI. N.C.: negative control scrambled miRNA. Scale bar represents 20 μm.

C. D145 has no inhibitory effects on GSK-3β

From the structural aspect, D145 (azathioprine) is a purine analogue [41], and a number of purine derivatives have been reported to have inhibitory effect on GSK-3β [42]. It has been reported that the suppression of GSK-3β produced profibrotic response [43]. Therefore, the anti-fibrotic effect of Azathioprine does not seem to be a result of Azathioprine-induced suppression of GSK-3β. Nevertheless, to make sure that Azathioprine does not affect the activity of GSK-3β at given concentration used for this study, I examined the phosphorylation status of GSK-3β in the presence of Azathioprine and Worthmannin, an inhibitor of Akt that inactivates the GSK-3β by phosphorylating the serine residue 9 of GSK-3β [44]. If Aziothioprine functions as an inhibitor of GSK-3β, it would increase the phosphorylation of GSK-3β even with the presence of Worthmannin. As shown in Figure 42, Worthmannin significantly decreased the phosphorylation of GSK-3β indicating that it actually activated GSK-3β by preventing phosphorylation of GSK-3β. However, pretreatment with Azathioprine failed to reverse the Wortmannin-induced downregulation of GSK-3β phosphorylation suggesting that Azathioprine at the given concentration did not inhibit (or increased the phosphorylation of) GSK-3β.

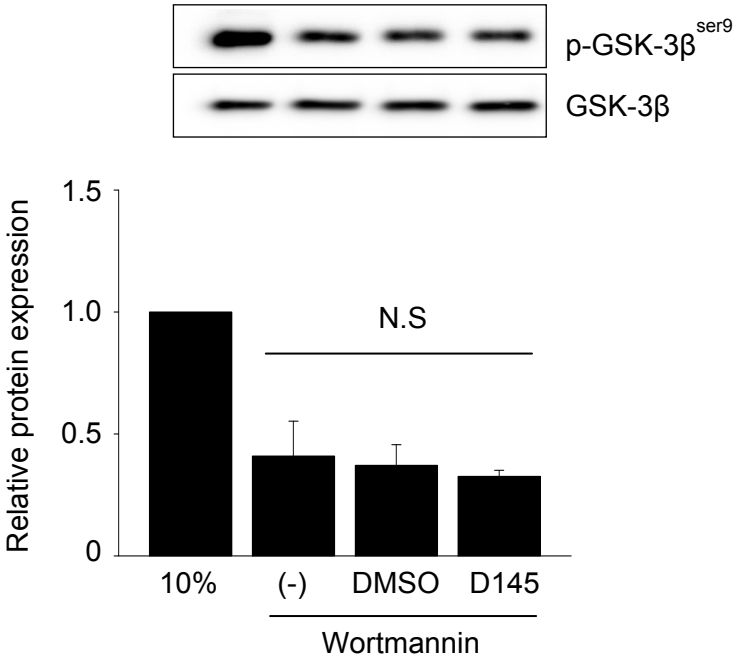

Figure 42. D145 has no effects on GSK-3β phosphorylation at Ser9. The cells were treated with Wortmannin (50nM) for 1hr in 10% FBS DMEM. After that, D145 (10μM) were added and incubated for 1hr. p-GSK-3β^{ser9} expression level was examined. Quantitative data were expressed as the means ± S.E.M. The similar results were obtained in at least 3 independent experiments.

13. Effect of D145 on TGF-β-induced activation of CFs

A. D145 inhibits the expression of CFs activation marker

To examine whether D145 could suppress TGF-β-induced activation of CFs similarly to miR-384-5p, the cells were treated with 10 μM D145 for 24 hours and exposed to 5 ng/ml TGF-β for an additional 24 hours. The D145 treatment significantly decreased the expression levels of collagen type I (Fig. 43). The negative effect of D145 on α-SMA expression was also confirmed by immunocytochemical staining (Fig. 44). These data indicated that TGF-β-induced CF activation was significantly attenuated by D145.

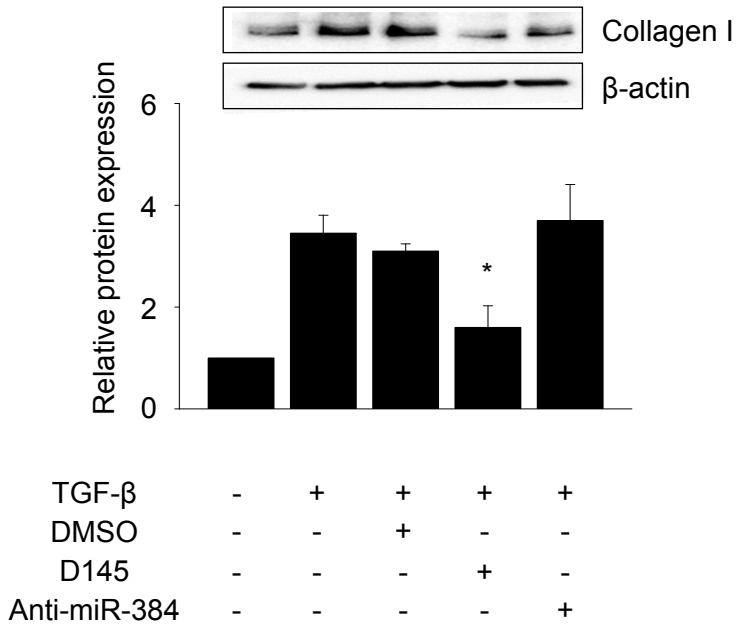

Figure 43. Effect of D145 on collagen type I expression in TGF-β-treated CFs. The cells were treated with 10 μM of D145 for 24 hours with or without the anti-miR-384-5p pretreatment. The expression of collagen type I (Collagen I) was examined by western blotting. Quantitative data were expressed as the means ± S.E.M. The similar results were obtained in at least 3 independent experiments. **p* <0.05 compared to TGF-β-treated control.

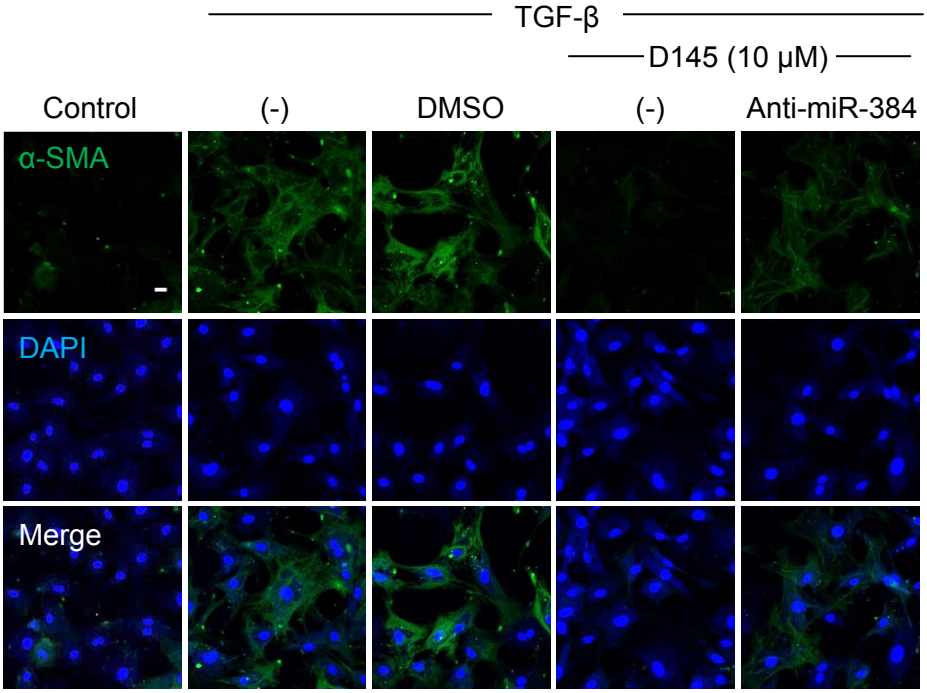

Figure 44. Immunocytochemical staining of α-SMA. The cells were treated with 10 μM of D145 for 24 hours with or without anti-miR-384-5p pretreatment. The expression of α-SMA was visualized by immunocytochemistry. Nuclei were stained with DAPI. Scale bar represents 20 μm.

B. D145 suppresses migration and contractility of TGF-β-stimulated CFs

The results of the migration analysis indicated that D145 significantly suppressed the migration of TGF-β-treated CFs (Fig. 45). The results of the collagen gel contraction analysis indicated that D145 significantly attenuated TGF-β-induced collagen contractility of the primary CFs (Fig. 46).

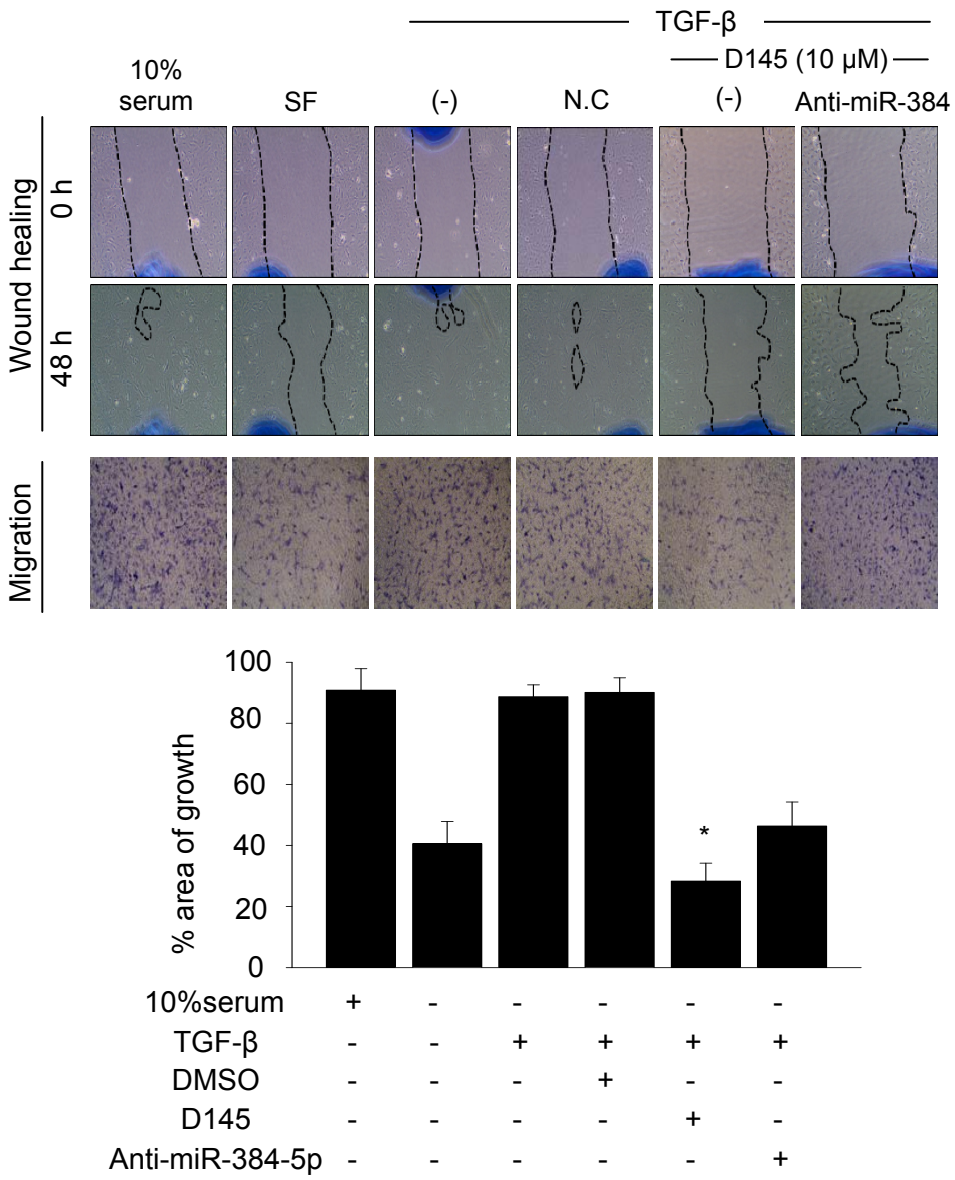

Figure 45. D145 attenuates migration of TGF-β-treated CFs. For wound healing assays, the cells were treated with 10 μM of D145 for 48 hours with or without anti-miR-384-5p pretreatment. The wound was created by scratching the surface of culture dish with a yellow pipette tip. The images of

wound were taken at time 0 and 48 hour. The area between the wound edges was measured and compared among groups. Quantitative data were expressed as the means ± S.E.M. The similar results were obtained in at least 3 independent experiments. *p <0.05 compared to TGF-β-treated control. For migration analysis, the cells were seeded in the upper chambers of Transwells and treated with 10 μM D145 for 24 hours with or without the anti-miR-384-5p pretreatment. The cells were further treated with TGF-β for an additional 24 hours. The migrated cells were stained with crystal violet. Scale bar represents 2 mm.

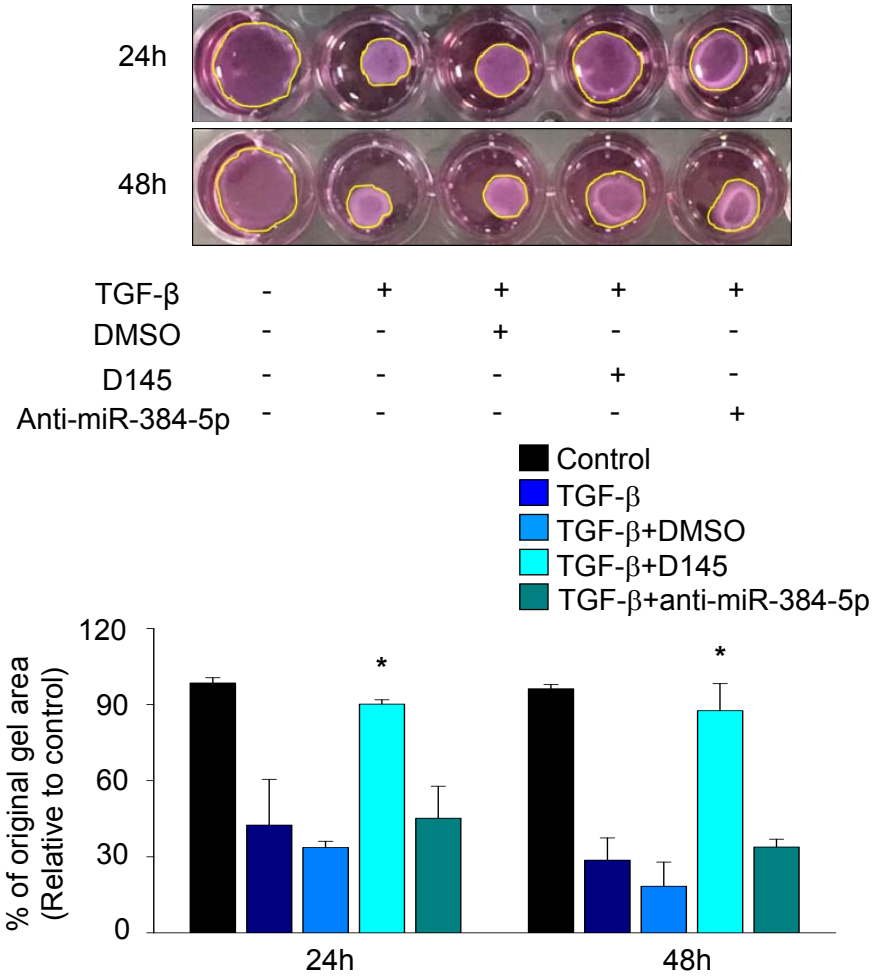

Figure 46. D145 attenuates collagen contractility of TGF-β-treated CFs. Cardiac fibroblast-containing collagen gels were serum-starved for 12 hours. Gels were stimulated with TGF-β (5 ng/ml) with or without D145 for 48 hours and photographed at 24 hour and 48 hour. The size of the gels were measured and analyzed. Quantitative data were expressed as the means ± S.E.M. The similar results were obtained in at least 3 independent experiments. **p* <0.05 compared to the TGF-β-treated control.

14. Effect of D145 on cardiac fibrosis following I/R-injury

A. D145 prevents the downregulation of miR-384-5p following I/R-injury

To investigate the therapeutic effect of D145 *in vivo*, D145 was intravenously (i.v.) injected via tail vein immediately after I/R-injury at a concentration of 10 μM. (The whole blood volume of an individual rat was approximated as 7% of the body weight.) [45] The expression level of miR-384-5p in the D145-treated group was well maintained for 2 weeks after the injury compared with that in the I/R-injured group (Fig. 47).

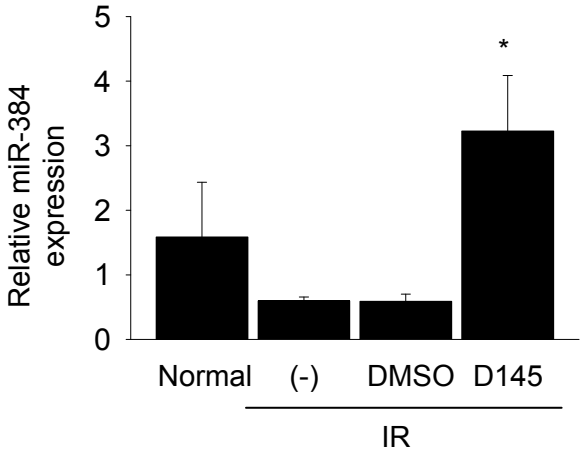

Figure 47. The expression of miR-384-5p in I/R-injured heart and D145 injected heart. The change of miR-384-5p expression following I/R-injury (14 days after the injury) with i.v. injection of D145 was detected by real time PCR. Quantitative data were expressed as the means ± S.E.M. of data collected from 5 animals. **p* <0.05 compared to I/R control.

B. D145 shows no serious *in vivo* adverse effect or toxicity

In contrast to miR-384-5p that was delivered by a local injection, D145 was systemically delivered via i.v. injection. Therefore, to evaluate the organ-specific and general toxicity of D145, multiple organs were weighed.[46] The data indicated that the weights of the organs were not significantly affected by D145, suggesting no serious *in vivo* adverse effects or toxicity of D145 (Fig. 48).

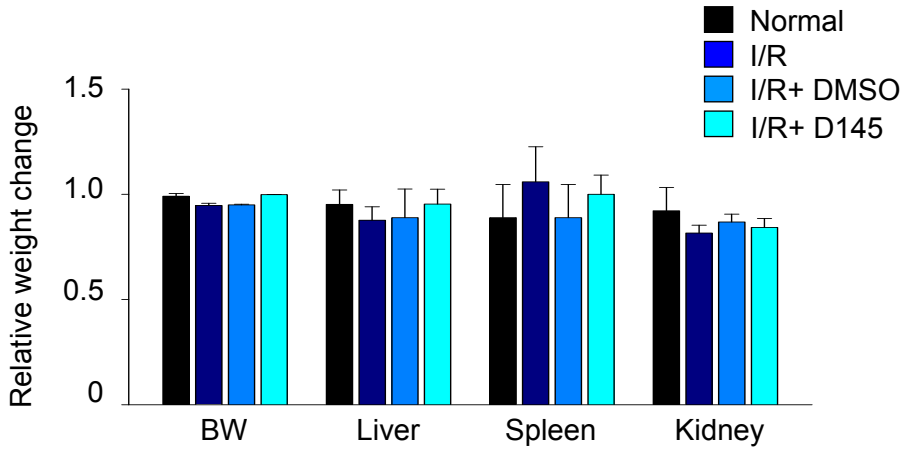

Figure 48. Body weight and organ weight of D145 injected cardiac I/R-injured rat. Body weight (BW) and organ (liver, spleen, and kidney) weight were measured to evaluate the general and organ-specific toxicity of D145. The organs were collected and weighed upon sacrifice of the animals at the end of the study. Data were expressed as the means ± S.E.M. of data collected from 5 animals.

C. D145 inhibits I/R-induced cardiac fibrosis by disrupting the circuit

Next, to examine whether D145 downregulated the expression levels of key receptors of interest as expected, the expression levels of Fzd1, Fzd2, Tgrbr1, and LRP6 were evaluated. The results showed that D145 significantly suppressed the expression of the receptors altogether (Fig. 49). Furthermore and most importantly, D145 significantly attenuated cardiac fibrosis (Fig. 50A), significantly decreasing the size of the fibrotic area (Fig. 50B) and preserving the LV wall thickness (Fig. 50C). Taken altogether, D145 significantly suppressed cardiac fibrosis by preventing the decrease in miR-384-5p in the heart following I/R-injury.

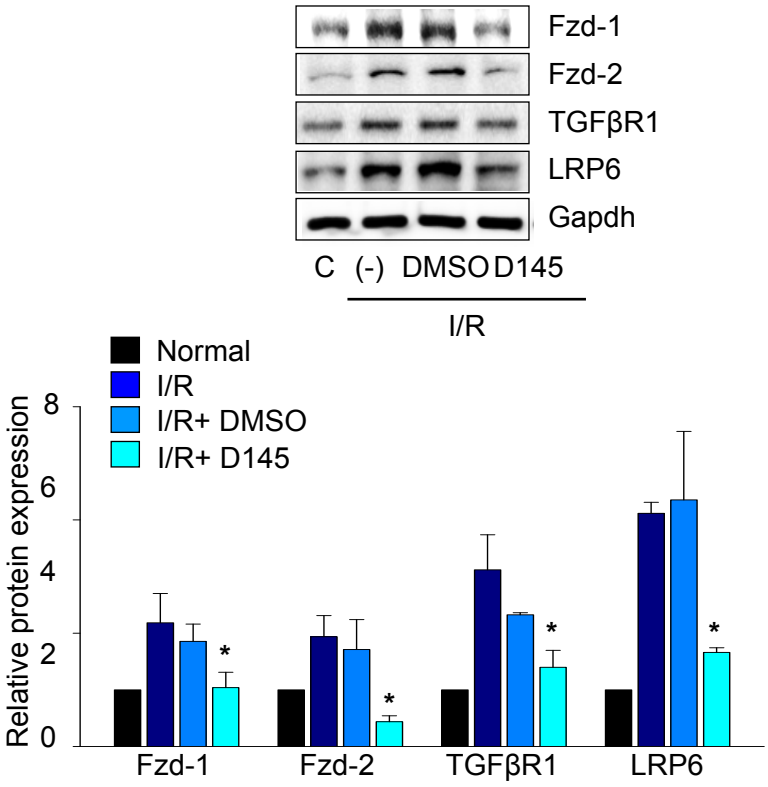

Figure 49. D145 decreases the expression of the receptors of the circuit following I/R-injury. The expression levels of key receptors in the I/R-injured heart with i.v. injection of D145 were detected by western blotting. Quantitative data were expressed as the means ± S.E.M. of at least 3 independent experiments. **p* <0.05 compared to I/R control.

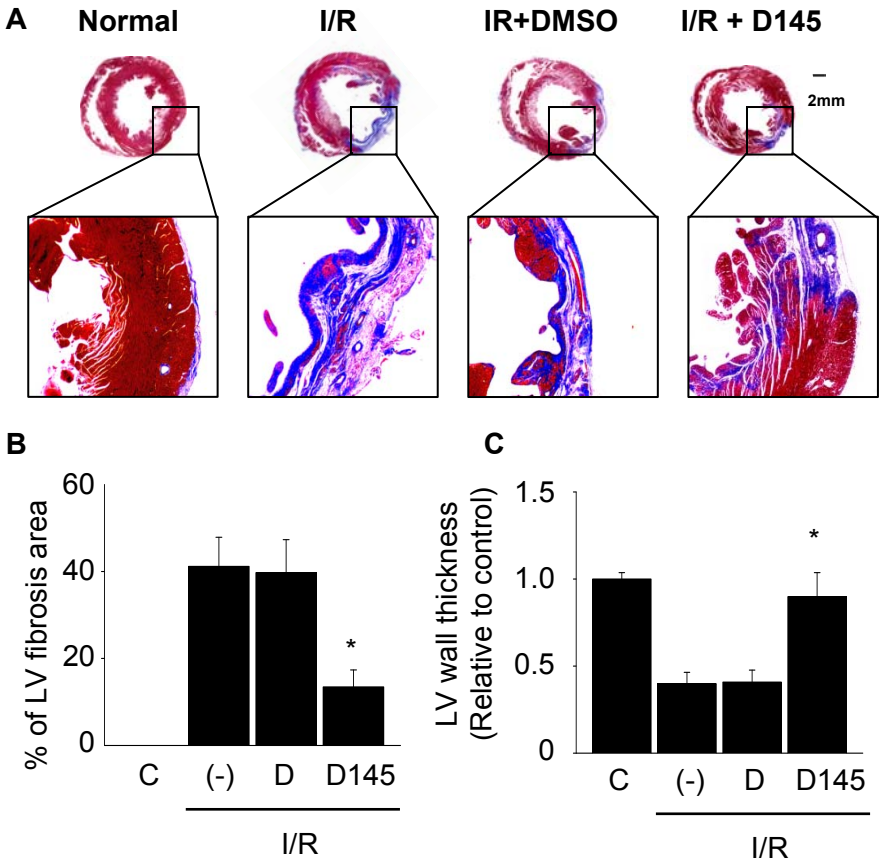

Figure 50. D145 attenuates cardiac fibrosis following I/R-injury. (A) Representative images of Masson's trichrome-stained sections demonstrating fibrosis. (B) The area of fibrosis and (C) left ventricular (LV) wall thickness were also measured. Quantitative data were expressed as the means ± S.E.M. of the data collected from 5 animals. **p* <0.05 compared to the I/R control.

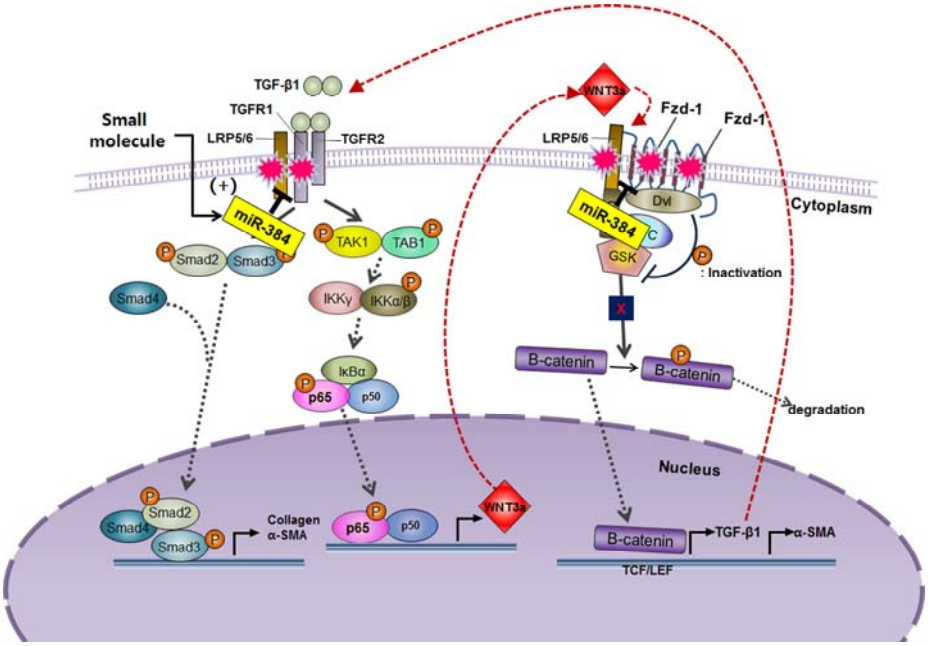

Figure 51. Model depicting the miR-384-5p-mediated regulation of the TGF-β/Wnt transactivation circuit in CFs. Model depicting miR-384-5p-mediated regulation of the TGF-β/Wnt transactivation circuit in CFs. The expression level of endogenous miR-384-5p is reduced by fibrogenic stimuli, increasing the expression of the key receptors (Fzd1, Fzd2, LRP6, and TGFβR1). This increase augments TGF-β-induced expression of the Wnt ligand Wnt3a, and consequently, Wnt3a further increases TGF-β production, establishing a TGF-β/Wnt transactivation circuit during CFs activation. Small molecule D145 augments the expression levels of endogenous miR-384-5p under fibrogenic stimuli, disrupting the transactivation circuit.

IV. DISCUSSION

Previous studies have provided circumstantial evidence of possible cross-talk between two major fibrogenic pathways by demonstrating that TGF-β can activate Wnt signaling and *vice versa* in different types of diseases involving myoFB formation.[7-9] Nevertheless, the existence of a transactivation circuit has not been examined nor experimentally confirmed in CF activation. In this study, I verified that the two pathways were indeed linked by demonstrating that exogenous TGF-β increased the production of Wnt3a in an NF-kB-dependent manner (Fig. 11) and that both neutralization of Wnt3a signaling (Fig. 15) and suppression of Wnt/β-catenin signaling (Fig. 5) attenuated the activation of the TGF-β autopositive feedback loop. Thus, the present study is the first to report the existence of a TGF-β/Wnt transactivation circuit in TGF-β-induced activation of CFs. However, a full confirmation of the existence of this circuit, especially *in vivo,* would be challenging.

To fully address the existence of such a circuit, a meticulously designed experimental strategy to distinguish at least the following 4 molecules is required: 1) initially applied exogenous TGF-β (referred to as primary TGF), 2) Wnt produced by primary TGF-β (referred to as primary Wnt), 3) secondary endogenous TGF-β produced by primary Wnt, and 4) secondary Wnt produced by secondary TGF-β. In the case of TGF-β, differential detection of primary and secondary TGF-β may be achieved by chemically

tagging primary TGF-β. However, the case of Wnt is more complicated because two different endogenous Wnts that are produced at different time periods need to be distinguished. Aside from the current technical feasibility of such an approach, the involvement of other growth factors and cytokines,[47, 48] which may or may not affect the TGF-β/Wnt transactivation circuit, makes an experimental confirmation of the existence of the circuit *in vivo* even more difficult. Therefore, providing direct *in vivo* evidence for a functioning TGF-β/Wnt transactivation circuit remains an issue that should be fully addressed in further studies.

Another significant finding of this study is the identification of miR-384-5p as an important regulator of the TGF-β/Wnt transactivation circuit. The identification of key miRNA(s) involved in the initiation and maintenance of the TGF-β/Wnt transactivation circuit was an integral part of the present study. Our data strongly suggested that miR-384-5p might have promoted increased expression of key receptors of TGF-β and Wnt signaling (i.e., Fzd1, Fzd2, TGFβR1, and LRP6 in the present study) by being decreased in response to fibrogenic stimulation *in vitro* and *in vivo* (Fig. 20). Consequently, the increased key receptor molecules initiate and maintain the TGF-β/Wnt transactivation circuit, contributing to the progression of cardiac fibrosis. Such speculation was indirectly verified by the observations of miR-384-5p-mediated suppression of CF activation *in vitro* (Fig. 21-28) and attenuation of

cardiac fibrosis *in vivo* (Fig. 29-31). Between the two miRNAs predicted to target the key receptors of TGF-β and Wnt signaling in the present study (Fig. 18), miR-384-5p is reportedly downregulated in ischemic diseases and in the failing heart,[49-51] whereas increased expression of miR-141-3p following ischemic preconditioning has been reported,[52] supporting the legitimacy of choosing miR-384-5p over miR-141-3p as a key miRNA that regulates the TGF-β/Wnt transactivation circuit.

Regarding the role of miR-384-5p in cardiovascular disease, one previous study reported a pro-apoptotic effect of miR-384-5p in cardiomyoblasts *in vitro*.[53] This particular study claimed that miR-384-5p increased the expression of caspase 3 and decreased the viability of cardiomyoblasts. However, the authors did not provide a detailed experimental procedure, particularly regarding the concentration of miRNA mimics used, making an evaluation and generalization of their findings difficult. Thus can only speculate that the observed effect of miR-384-5p is cell-type specific or that the effect is an artifact caused by an improper concentration of miRNA mimics. Interestingly, even the aforementioned study demonstrated that the expression of miR-384-5p decreased by 60% in the ischemic myocardium. Nevertheless, investigating the effects of miR-384-5p on different types of cardiac cells other than fibroblasts to better comprehend the role of miR-384-5p in the cardiovascular system will be a meaningful goal for further studies.

The most clinically relevant finding of the present study is the prevention of cardiac fibrosis mediated by a small molecule, D145. To bypass current limitations, such as low cellular uptake, off-target effects, and instability in serum, of directly applying exogenous miRNAs *in vivo*,[36] small-molecule-mediated regulation of endogenous miR-384-5p was utilized as an alternative strategy to modulate the expression levels of the key receptors involved in the TGF-β/Wnt transactivation circuit *in vivo*. The selected small molecule, D145, significantly attenuated TGF-β-induced downregulation of miR-384-5p (Fig. 35), and furthermore, D145 significantly suppressed TGF-β-induced activation of CFs *in vitro* (Fig. 42-45).

Regarding the mechanism of the D145-mediated prevention of endogenous miR-384-5p downregulation induced by fibrogenic stimulation, the results of the promoter analysis using the 3-kb promoter sequence of rno-miR-384-5p strongly suggested that the effect of D145 was not due to increased transcription of miR-384-5p (Fig. 36). However, there is a possibility that the distal promoter(s) of miR-384-5p that are affected by D145 may exist outside of the promoter range investigated in the present study because functional distal promoters of miRNA can be situated far upstream from the miRNA coding sequence. For example, a powerful distal promoter of has-miR-648 is reportedly 43.6 kb upstream of the coding sequence.[54]

If the effect of D145 is not dependent on transcriptional activity, other possibilities that have not been explored in the present study include miRNA

stability (degradation) regulation [39] or increased processing of primary miRNA (pri-mRNA) to mature miRNA [40] by D145. However, to validate or rule out these possibilities, further experiments are needed to examine the effects of D145 on the expression levels and functions of related enzymes such as miRNA-degrading exoribonucleases [55] and pri-miRNA-processing RNase III enzymes.[56] Furthermore, the present study is limited in that it does not address how fibrogenic stimuli, such as TGF-β, downregulate the endogenous expression of miR-384-5p. These mechanistic details will provide critical information for clarifying the underlying mechanism of D145.

In addition to suppressing TGF-β-induced activation of CFs *in vitro*, D145 also significantly attenuated cardiac fibrosis following I/R-injury *in vivo* (Fig. 49). The result of the measurement of LV wall thickness and the LV fibrotic area (Fig. 31 and 49) indicated that both miR-384-5p and D145 were effective to attenuate I/R-induced cardiac fibrosis. However, only two parameters are not enough to fully assess the anti-fibrotic efficacies of miR-384-5p and D145, and therefore, it is difficult to simply state that the efficacies of miR-384-5p and D145 are comparable with the data I provide in this study. However, assuming that the efficacies of miR-384-5p and D145 are quite similar at the given concentration used in the present study, D145 may be a clinically preferable means to control fibrosis because its clinical application would be much simpler than that of exogenous miR-384-5p.

Although the D145-mediated attenuation of endogenous miR-384-5p (Fig. 46) and downregulation of key receptors (Fig. 48) following I/R-injury indicated that the anti-fibrotic effect of D145 was mediated by the disruption of the TGF-β/Wnt transactivation circuit as proposed, additional unforeseen mechanisms may function *in vivo*. Unlike *in vitro* conditions where biological variables are well-controlled and minimized (e.g., single cell type and single treatment), *in vivo* conditions include a wide variety of cells and a number of soluble factors. Therefore, unexpected mechanism(s) of action may also contribute to the outcomes of an *in vivo* experiment. Consequently, consideration of possible mechanisms, other than disruption of the TGF-β/Wnt transactivation circuit in CFs, that might have contributed to the observed anti-fibrotic effect of D145 will be required to interpret the outcomes correctly and to design further *in vivo* studies adequately.

Assuming that D145 disrupts the TGF-β/Wnt transactivation circuit so that Wnt protein production from CFs is downregulated, the very first possible effect is that the downregulation of Wnt signaling has a positive effect on cardiac cells other than CFs.[57] Downregulation of β-catenin enhances resident precursor cell differentiation and attenuates ischemic cardiac remodeling,[58] and a small-molecule inhibitor of Wnt signaling improves the contractile function in the infarcted heart.[59] Furthermore, blocking Fzd-mediated Wnt signaling by using either a soluble decoy for the Wnt protein[60] or siRNA that

is specific to Fzd [61] prevents apoptosis of cardiomyocytes, supporting the possibility that D145 acts as a regulator of a Wnt protein-based niche in the I/R-injured heart. Another possibility is based on the pharmaceutical nature of D145. The identity of D145 is azathioprine, a well-known immunosuppressive agent,[38] and the immunosuppressive effect of azathioprine is mainly achieved via inhibition of CD28-mediated signaling, including NF-kB.[62] CD28 is a homodimeric stimulatory receptor that is expressed on T cells and mediates co-stimulation of T cells.[63] Recently, studies have reported that inhibition of T cell co-stimulation[64] or CD28 deficiency[65] has a protective effect on pressure overload-induced congestive heart failure. Therefore, D145 may protect the I/R-injured heart by not only disrupting the TGF-β/Wnt transactivation circuit but by also suppressing the immune response following I/R-injury. However, these possibilities will remain speculative until they are experimentally confirmed.

Ⅴ. CONCLUSION

The present study has provided strong evidence of a TGF-β-Wnt transactivation circuit in CFs and has identified miR-384-5p as a key regulator of the circuit (Fig. 50). In the clinical context, the results of this study indicate that modulating a key miRNA targeting multiple fibrogenic mediators can be an effective means to control cardiac fibrosis and that small-molecule-mediated regulation of endogenous miRNA has significant therapeutic potential as a clinically viable alternative to direct application of exogenous miRNAs. To fully address the unanswered issues, further studies are warranted.

References

1. Baum J, Duffy HS. Fibroblasts and myofibroblasts: what are we talking about? J Cardiovasc Pharmacol 2011;57:376-379.
2. Talman V, Ruskoaho H. Cardiac fibrosis in myocardial infarction-from repair and remodeling to regeneration. Cell Tissue Res 2016;365:563-581.
3. Chablais F, Jazwinska A. The regenerative capacity of the zebrafish heart is dependent on TGF-β signaling. Development 2012;139:1921-1930.
4. Dobaczewski M, Chen W, Frangogiannis NG. Transforming growth factor (TGF)-β signaling in cardiac remodeling. J Mol Cell Cardiol 2011;51:600-606.
5. Meng XM, Nikolic-Paterson DJ, Lan HY. TGF-β: the master regulator of fibrosis. Nat Rev Nephrol 2016;12:325-338.
6. Leask A. TGF-β, cardiac fibroblasts, and the fibrotic response. Cardiovasc Res 2007;74:207-212.
7. Akhmetshina A, Palumbo K, Dees C, Bergmann C, Venalis P, Zerr P, et al. Activation of canonical Wnt signalling is required for TGF-β-mediated fibrosis. Nat Commun 2012;3:735.
8. Carthy JM, Garmaroudi FS, Luo Z, McManus BM. Wnt3a induces myofibroblast differentiation by upregulating TGF-β signaling

through SMAD2 in a β-catenin-dependent manner. PLoS One 2011;6:e19809.

9. Blyszczuk P, Muller-Edenborn B, Valenta T, Osto E, Stellato M, Behnke S, et al. Transforming growth factor-β-dependent Wnt secretion controls myofibroblast formation and myocardial fibrosis progression in experimental autoimmune myocarditis. Eur Heart J 2017;38:1413-1425.
10. Ha M, Kim VN. Regulation of microRNA biogenesis. Nat Rev Mol Cell Biol 2014;15:509-524.
11. Xu P, Guo M, Hay BA. MicroRNAs and the regulation of cell death. Trends Genet 2004;20:617-624.
12. Ivey KN, Srivastava D. MicroRNAs as regulators of differentiation and cell fate decisions. Cell Stem Cell 2010;7:36-41.
13. Hwang HW, Mendell JT. MicroRNAs in cell proliferation, cell death, and tumorigenesis. Br J Cancer 2007;96 Suppl:R40-44.
14. Hashimoto Y, Akiyama Y, Yuasa Y. Multiple-to-multiple relationships between microRNAs and target genes in gastric cancer. PLoS One 2013;8:e62589.
15. Lijnen PJ, Petrov VV, Fagard RH. Induction of cardiac fibrosis by transforming growth factor-β(1). Mol Genet Metab 2000;71:418-435.
16. Zanetta L, Marcus SG, Vasile J, Dobryansky M, Cohen H, Eng K, et al. Expression of Von Willebrand factor, an endothelial cell marker, is

up-regulated by angiogenesis factors: a potential method for objective assessment of tumor angiogenesis. Int J Cancer 2000;85:281-288.

17. Shinde AV, Humeres C, Frangogiannis NG. The role of α-smooth muscle actin in fibroblast-mediated matrix contraction and remodeling. Biochim Biophys Acta 2017;1863:298-309.
18. Speiser B, Weihrauch D, Riess CF, Schaper J. The extracellular matrix in human cardiac tissue. Part II: Vimentin, laminin, and fibronectin. Cardioscience 1992;3:41-49.
19. Lijnen P, Petrov V. Transforming growth factor-β 1-induced collagen production in cultures of cardiac fibroblasts is the result of the appearance of myofibroblasts. Methods Find Exp Clin Pharmacol 2002;24:333-344.
20. Kondo S, Kagami S, Urushihara M, Kitamura A, Shimizu M, Strutz F, et al. Transforming growth factor-β1 stimulates collagen matrix remodeling through increased adhesive and contractive potential by human renal fibroblasts. Biochim Biophys Acta 2004;1693:91-100.
21. Komiya Y, Habas R. Wnt signal transduction pathways. Organogenesis 2008;4:68-75.
22. Boutros M, Paricio N, Strutt DI, Mlodzik M. Dishevelled activates JNK and discriminates between JNK pathways in planar polarity and wingless signaling. Cell 1998;94:109-118.

23. De A. Wnt/Ca^{2+} signaling pathway: a brief overview. Acta Biochim Biophys Sin (Shanghai) 2011;43:745-756.
24. MacDonald BT, Tamai K, He X. Wnt/β-catenin signaling: components, mechanisms, and diseases. Dev Cell 2009;17:9-26.
25. Kikuchi A, Yamamoto H, Sato A, Matsumoto S. New insights into the mechanism of Wnt signaling pathway activation. Int Rev Cell Mol Biol 2011;291:21-71.
26. Fredriksson R, Lagerstrom MC, Lundin LG, Schioth HB. The G-protein-coupled receptors in the human genome form five main families. Phylogenetic analysis, paralogon groups, and fingerprints. Mol Pharmacol 2003;63:1256-1272.
27. Blankesteijn WM, Essers-Janssen YP, Verluyten MJ, Daemen MJ, Smits JF. A homologue of Drosophila tissue polarity gene frizzled is expressed in migrating myofibroblasts in the infarcted rat heart. Nat Med 1997;3:541-544.
28. Laeremans H, Hackeng TM, van Zandvoort MA, Thijssen VL, Janssen BJ, Ottenheijm HC, et al. Blocking of frizzled signaling with a homologous peptide fragment of wnt3a/wnt5a reduces infarct expansion and prevents the development of heart failure after myocardial infarction. Circulation 2011;124:1626-1635.
29. Zhang YE. Non-Smad Signaling Pathways of the TGF-β Family. Cold Spring Harb Perspect Biol 2017;9.

30. Choi ME, Ding Y, Kim SI. TGF-β signaling via TAK1 pathway: role in kidney fibrosis. Semin Nephrol 2012;32:244-252.
31. Karin M. How NF-κB is activated: the role of the IκB kinase (IKK) complex. Oncogene 1999;18:6867-6874.
32. Natarajan K, Singh S, Burke TR, Jr., Grunberger D, Aggarwal BB. Caffeic acid phenethyl ester is a potent and specific inhibitor of activation of nuclear transcription factor NF-κB. Proc Natl Acad Sci U S A 1996;93:9090-9095.
33. Handeli S, Simon JA. A small-molecule inhibitor of Tcf/β-catenin signaling down-regulates PPARγ and PPAR δ activities. Mol Cancer Ther 2008;7:521-529.
34. Shi Y, Massague J. Mechanisms of TGF-β signaling from cell membrane to the nucleus. Cell 2003;113:685-700.
35. MacDonald BT, He X. Frizzled and LRP5/6 receptors for Wnt/β-catenin signaling. Cold Spring Harb Perspect Biol 2012;4.
36. Pecot CV, Calin GA, Coleman RL, Lopez-Berestein G, Sood AK. RNA interference in the clinic: challenges and future directions. Nat Rev Cancer 2011;11:59-67.
37. Hwang KC, Kim JY, Chang W, Kim DS, Lim S, Kang SM, et al. Chemicals that modulate stem cell differentiation. Proceedings of the National Academy of Sciences of the United States of America 2008;105:7467-7471.

38. Maltzman JS, Koretzky GA. Azathioprine: old drug, new actions. J Clin Invest 2003;111:1122-1124.
39. Bail S, Swerdel M, Liu H, Jiao X, Goff LA, Hart RP, et al. Differential regulation of microRNA stability. RNA 2010;16:1032-1039.
40. Conrad T, Marsico A, Gehre M, Orom UA. Microprocessor activity controls differential miRNA biogenesis In Vivo. Cell Rep 2014;9:542-554.
41. Sharma S, Mehndiratta S, Kumar S, Singh J, Bedi PM, Nepali K. Purine Analogues as Kinase Inhibitors: A Review. Recent Pat Anticancer Drug Discov 2015;10:308-341.
42. Eldar-Finkelman H, Martinez A. GSK-3 Inhibitors: Preclinical and Clinical Focus on CNS. Front Mol Neurosci 2011;4:32.
43. Lal H, Ahmad F, Zhou J, Yu JE, Vagnozzi RJ, Guo Y, et al. Cardiac fibroblast glycogen synthase kinase-3β regulates ventricular remodeling and dysfunction in ischemic heart. Circulation 2014;130:419-430.
44. Inoue N, Iwasa T, Fukunaga K, Matsukado Y, Miyamoto E. Phosphorylation and inactivation of brain glycogen synthase by a multifunctional calmodulin-dependent protein kinase. J Neurochem 1987;48:981-988.
45. Lee HB, Blaufox MD. Blood volume in the rat. J Nucl Med

1985;26:72-76.

46. Michael B, Yano B, Sellers RS, Perry R, Morton D, Roome N, et al. Evaluation of organ weights for rodent and non-rodent toxicity studies: a review of regulatory guidelines and a survey of current practices. Toxicol Pathol 2007;35:742-750.
47. Kendall RT, Feghali-Bostwick CA. Fibroblasts in fibrosis: novel roles and mediators. Front Pharmacol 2014;5:123.
48. Borthwick LA, Wynn TA, Fisher AJ. Cytokine mediated tissue fibrosis. Biochim Biophys Acta 2013;1832:1049-1060.
49. Muthusamy S, DeMartino AM, Watson LJ, Brittian KR, Zafir A, Dassanayaka S, et al. MicroRNA-539 is up-regulated in failing heart, and suppresses O-GlcNAcase expression. J Biol Chem 2014;289:29665-29676.
50. Zhai F, Zhang X, Guan Y, Yang X, Li Y, Song G, et al. Expression profiles of microRNAs after focal cerebral ischemia/reperfusion injury in rats. Neural Regen Res 2012;7:917-923.
51. Sun G, Hu H, Tian X, Yue J, Yu H, Yang X, et al. Identification and analysis of microRNAs in the left ventricular myocardium of two-kidney one-clip hypertensive rats. Mol Med Rep 2013;8:339-344.
52. Lee ST, Chu K, Jung KH, Yoon HJ, Jeon D, Kang KM, et al. MicroRNAs induced during ischemic preconditioning. Stroke 2010;41:1646-1651.

53. Bao Y, Lin C, Ren J, Liu J. MicroRNA-384-5p regulates ischemia-induced cardioprotection by targeting phosphatidylinositol-4,5-bisphosphate 3-kinase, catalytic subunit δ (PI3K p110δ). Apoptosis 2013;18:260-270.
54. Li C, Gonsalves CS, Eiymo Mwa Mpollo MS, Malik P, Tahara SM, Kalra VK. MicroRNA 648 Targets ET-1 mRNA and is cotranscriptionally regulated with MICAL3 by PAX5. Mol Cell Biol 2015;35:514-528.
55. Zhang Z, Qin YW, Brewer G, Jing Q. MicroRNA degradation and turnover: regulating the regulators. Wiley Interdiscip Rev RNA 2012;3:593-600.
56. Gregory RI, Yan KP, Amuthan G, Chendrimada T, Doratotaj B, Cooch N, et al. The Microprocessor complex mediates the genesis of microRNAs. Nature 2004;432:235-240.
57. Hermans KC, Daskalopoulos EP, Blankesteijn WM. Interventions in Wnt signaling as a novel therapeutic approach to improve myocardial infarct healing. Fibrogenesis Tissue Repair 2012;5:16.
58. Zelarayan LC, Noack C, Sekkali B, Kmecova J, Gehrke C, Renger A, et al. β-Catenin downregulation attenuates ischemic cardiac remodeling through enhanced resident precursor cell differentiation. Proc Natl Acad Sci U S A 2008;105:19762-19767.
59. Sasaki T, Hwang H, Nguyen C, Kloner RA, Kahn M. The small

molecule Wnt signaling modulator ICG-001 improves contractile function in chronically infarcted rat myocardium. PLoS One 2013;8:e75010.

60. Zhang Z, Deb A, Zhang Z, Pachori A, He W, Guo J, et al. Secreted frizzled related protein 2 protects cells from apoptosis by blocking the effect of canonical Wnt3a. J Mol Cell Cardiol 2009;46:370-377.
61. Zhou SS, He F, Chen AH, Hao PY, Song XD. Suppression of rat Frizzled-2 attenuates hypoxia/reoxygenation-induced Ca^{2+} accumulation in rat H9c2 cells. Exp Cell Res 2012;318:1480-1491.
62. Tiede I, Fritz G, Strand S, Poppe D, Dvorsky R, Strand D, et al. CD28-dependent Rac1 activation is the molecular target of azathioprine in primary human CD4+ T lymphocytes. J Clin Invest 2003;111:1133-1145.
63. Beyersdorf N, Kerkau T, Hunig T. CD28 co-stimulation in T-cell homeostasis: a recent perspective. Immunotargets Ther 2015;4:111-122.
64. Kallikourdis M, Martini E, Carullo P, Sardi C, Roselli G, Greco CM, et al. T cell costimulation blockade blunts pressure overload-induced heart failure. Nat Commun 2017;8:14680.
65. Wang H, Kwak D, Fassett J, Hou L, Xu X, Burbach BJ, et al. CD28/B7 Deficiency Attenuates Systolic Overload-Induced Congestive Heart Failure, Myocardial and Pulmonary Inflammation,

and Activated T Cell Accumulation in the Heart and Lungs. Hypertension 2016;68:688-696.

ABSTRACT (in Korean)

TGF-β/Wnt 교차활성회로를 다중 표적하는 마이크로 RNA 384-5p 의 조절을 통한 심근섬유화의 억제

<지도교수 박 종 철>

연세대학교 대학원 의과학과

서 향 희

심근섬유화는 (cardiac fibrosis) 심근의 손상으로 인한 심실기능이상 (ventricular dysfunction) 및 심부전증이 (heart failure) 진행되는 과정에서 일반적으로 동반되는 증상이다. 심근섬유화의 초기에 발생하는 일련의 과정 중 중요한 것은 심근손상 시 생성되는 TGF-β 등과 같은 사이토카인에 의한 심근섬유아세포 (cardiac fibroblast)의 근섬유아세포로의 (myofibroblast) 활성화가 있으며 이러한 심근 섬유아세포의 활성을

억제하는 것은 심근섬유화의 억제를 위한 효과적인 방법으로 알려져 있다. 본 연구에서는 심근섬유화에 중요한 역할을 하는 것으로 알려진 바 있는 TGF-β 신호와 Wnt 신호가 심근섬유아세포의 활성화 과정에 있어서 교차활성화회로를 (TGF-β/Wnt transactivation circuit) 구성한다는 것을 실험적으로 입증하고 또한 이 회로를 구성하고 있는 다수의 수용체를 동시에 표적하는 마이크로 RNA를 조절해 심근섬유화를 효과적으로 억제할 수 있다는 것을 확인하였다. 주요 결과를 보면 TGF-β처리는 심근섬유아세포에서 Wnt 리간드의 생성을 증가시켜 TGF-β의 자가양성 되먹임 루프를 (auto positive feedback loop) 활성화 시켰으며 해당 Wnt 리간드의 중화항체 (neutralizing antibodies) 처리를 통해 이러한 양성 되먹임 루프의 활성이 억제되는 것을 확인하였다. 또한 본 연구를 통해 마이크로 RNA 384-5p가 TGF-β/Wnt 교차활성화회로를 구성하는 주요 수용체를 동시에 표적하는 주요 마이크로 RNA 중 하나임을 입증하였으며 이의 조절을 통해 TGF-β에 의한 심근 섬유아세포의 활성화 및 허혈-재관류 (ischemia-reperfusion) 손상에 의한 심근섬유화를 효과적으로 억제할 수 있음을 확인하였다. 추가적으로, 외인적 마이크로 RNA의 생체 내 전달이 가지고 있는 한계점의 극복을 위해 저분자화합물을 이용해

내인적 마이크로 RNA 384-5p의 병리학적 감소를 억제한 결과 이 역시 심근 섬유아세포의 활성화 및 심근섬유화를 억제하는 것을 확인하였다. 본 연구의 결과는 TGF-β/Wnt 교차활성화회로를 구성하는 주요 인자를 동시에 표적하는 마이크로 RNA의 조절을 통해 심근섬유화를 효과적으로 억제할 수 있다는 것을 보여주며 본 연구를 통해 제시된 병리학적 마이크로 RNA의 조절을 통한 심근섬유화 억제 개념은 추가적인 실험적 검증 및 보완 연구를 통해 임상적 적용 가능성 등을 확인할 만한 충분한 가치가 있다고 사료된다.

핵심되는 말: 마이크로RNA-384-5p, 심장섬유화, 저분자 화합물